JOURNAL OF MATERIALS SCIENCE: MATERIALS IN ELECTRONICS 4 (1993) 1–28

Review
Impurity-induced disordering in III–V multi-quantum wells and superlattices

I. HARRISON
Department of Electrical and Electronic Engineering, University of Nottingham, Nottingham NG7 2RD, UK

Impurity-induced disordering seems to be a general phenomenon affecting all III–V materials. This paper reviews this phenomenon. Before the available data on impurity-induced disordering is discussed, the diffusion mechanisms for the dopants are briefly reviewed, and for silicon-doped material a more detailed discussion is provided because of its technological importance. Moreover, there has been no critical review of the recent progress in silicon diffusion mechanisms. In zinc-diffused multi-quantum wells and superlattices the mechanism for the enhancement of the interdiffusion seems to be primarily by the fast diffusion of group III interstitials whose concentration has been significantly increased over their equilibrium value by the diffusion of the dopant. For silicon impurity-induced disorder the situation is less clear. However, it is certain that the effect of the position of the Fermi level on the native defect concentrations plays a significant role in the disordering mechanism. The study of the other dopants which cause diffusion-induced disordering is less advanced. For n-type dopants there is an argument which suggests that they all have a common cause, namely the increase in the group III triply charged vacancy which is caused by the increase in the Fermi energy. This will be explored in this review. A brief discussion of ion implantation-induced disordering is also provided. This essentially provides a bibliography of the past work in this field. It is clear, for at least one dopant, that there needs to be some damage to the crystal before the enhancement of the interdiffusion occurs. However, for other dopants too much damage reduces the enhancement of the intermixing.

Contents

1. Introduction

It has been known for a long time that the self-diffusion of group III and group V atoms in III–V semiconductors is slow when compared with the diffusion of other dopants. With the advent of modern epitaxy techniques, the slow self-diffusion has enabled the growth of abrupt junctions of differing semiconductors. For example, single crystals containing layers of GaAs and AlAs can be grown. The width of these layers can be as small as one monolayer or as large as the grower wishes. This has therefore provided device engineers with a new dimension in the designing of novel electronic device structures. The band gap within a crystal can be changed locally so that the performance of a device can be optimized. One example of this is the modulation-doped field-effect transistor. In this device, the discontinuities in the conduction band or valence band are used to obtain a two-dimensional electron or hole gas. This two-dimensional carrier sheet is removed spatially from the donor or acceptor dopants and, therefore, the carrier

0957–4522

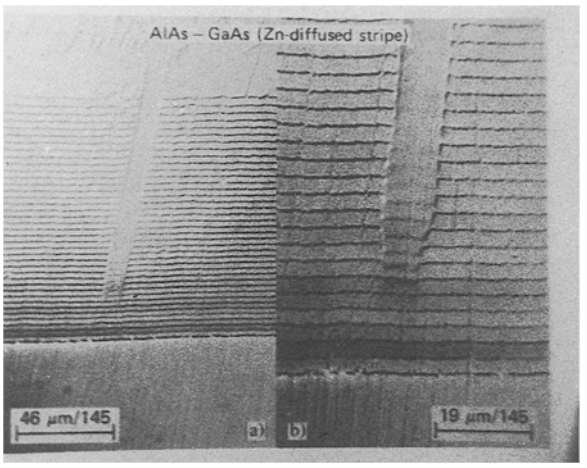

Figure 1 Bevel section of zinc-diffused GaAs–$Al_{0.77}Ga_{0.33}As$ superlattice (l_z = 4.5 nm, L_b = 15 nm) performed at 575 °C for 10 min. The diffusion has been performed through a 10 μm stripe opened up in a Si_3N_4 diffusion mask. This clearly shows the intermixing associated with the diffusion of the zinc (after Laidig *et al.* [2]). (Reproduced with the permission of the American Institute of Physics.)

mobility in these devices is greater than that of the bulk material since the electronic scattering by impurity atoms has been minimized.

Owing to the low diffusivity of the group III and group V atoms, the structures briefly described above are remarkably stable to heat treatment. For example, a 2 μm superlattice consisting of layers of GaAs and AlAs, each layer being 50 nm thick, only shows a slight degradation of the interface between the layers, after a 700 °C 17 h thermal anneal [1]. In 1981 Laidig *et al.* [2], while attempting to dope a superlattice P type by diffusing zinc into it, discovered by accident an effect now known as impurity-induced disordering (IID). Wherever the zinc had diffused the interdiffusion of the layers had significantly increased. This is clearly shown in Fig. 1 which shows a bevel section of a sample which has been zinc-diffused for 10 min at 575 °C through an opening in a diffusion mask. Wherever the zinc has diffused the resulting material is a ternary alloy whose composition is the average of the superlattice.

The use of this effect in optoelectronics was immediately recognised. By selectively disordering a superlattice lateral changes in refractive index can be achieved and optical waveguides manufactured. This use has led to the current high level of interest in impurity-induced disordering. Since the first discovery of the effect in zinc-diffused GaAs–GaAlAs superlattices, many other dopants have been found to cause it. Perhaps one of the most important technologically is silicon. In addition, the effect has been seen in other III–V superlattice systems, such as InGaAs–InP, and so appears to be a general effect associated with III–V superlattices. Also, the enhancement of the interdiffusion may affect either or both sublattices. This paper concentrates on attempting to review the mechanisms underlying the effect. However, before discussing these in more detail, there are several points to raise.

There must be a close relationship between the diffusion mechanisms of the dopants in the binary or ternary alloys and the disordering mechanism. The two cannot be unconnected and there should be no discussion of either topic without reference to the other. The mechanism assigned to the diffusion of a dopant in the III–V semiconductor must explain directly or indirectly the impurity-induced disordering effect. This review gives only an insight into the diffusion mechanism of a particular dopant. For a more detailed discussion of the topic the reader is directed to the book written by Tuck [3]. The exception to this is the diffusion of silicon in GaAs. In the last few years a substantial amount of work on the diffusion mechanisms of silicon has been reported. This work was not reviewed by Tuck [3] and so a detailed critique is given here.

In the following sections the effect of diffusing dopants into different superlattice systems is described. The GaAlAs system is the only superlattice which has been extensively studied, and so in the underlying discussions it will be treated first. If any other work on other systems has been reported it will be discussed afterwards. Preceding all the discussions on the superlattices the diffusion mechanisms which occur in ternary and binary compounds will be reviewed briefly.

2. Thermal annealing of nominally undoped III–V superlattices

2.1. GaAs–AlAs

The thermal interdiffusion of GaAs–$Ga_xAl_{1-x}As$ has been studied extensively [4–31]. The usual experimental method of investigating the degree of intermixing has been photoluminescence. To obtain a figure for the interdiffusion coefficient Fick's law is usually assumed, and the diffusion coefficient is assumed to be independent of the concentration value even though early work showed that a concentration-dependent interdiffusion coefficient was necessary [4, 5]. The close relationship between interdiffusion and self-diffusion cannot be forgotten. For GaAs, there is a small amount of self-diffusion data [6–8]; however, for the ternary $Al_xGa_{1-x}As$ and AlAs no such data are available. The connection between self- and interdiffusion was recognised by Tan and Gösele [9] who plotted on the same Arrhenius diagram the available data for gallium self-diffusion in GaAs with the available interdiffusion data of the GaAs–AlGaAs system. In addition, they plotted data derived from the silicon work of Mei *et al.* [10]. The three sets of data appear to lie on the same straight line which is given by

$$D_{Ga} = 2.9 \times 10^8 \exp \frac{-6eV}{k_b T} \text{ cm}^{-2}\text{s}^{-1} \quad (1)$$

From the work of Mei *et al.* [10], Tan and Gösele [9, 11] concluded that the enhancement of the gallium diffusivity under silicon and intrinsic doping is governed by a triply negatively charged gallium vacancy. The large difference between the interdiffusion coefficient of the intrinsic multi-quantum well structures and the silicon-doped multi-quantum well structures is accounted for in this model by the increased solubility of the V_{Ga}^{-3} in n-type material (see section 6 below). Since the process used to explain the interdiffusion

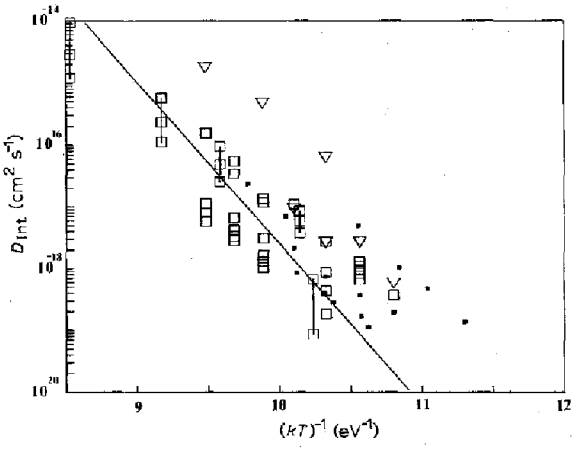

Figure 2 Arrhenius plot of the interdiffusion coefficient of AlGaAs–GaAs. The data used come from the work of Guido *et al.* [13], Chang and Koma [4], Fleming *et al.* [5], Schleslinger and Kuech [29], Ralston,*et al.* [31] and Hsieh *et al.* [17]. Equation 1 is represented by the line; (■) sample capped with SiN_x, (□) no cap, (▽) SiO_2 cap.

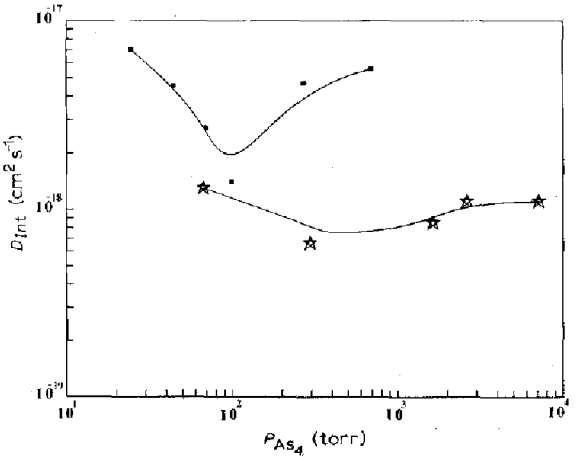

Figure 3 Interdiffusion coefficient as a function of As_4 pressure: (■) data of Guido *et al.* [13], (✡) data of Furuya *et al.* [14].

depends on the electron concentration and not the dopant species this explanation should be applicable to all n-type dopants.

In the analysis described above, interdiffusion data are available for temperatures only in the mid-range (800–1000 °C). At low temperatures (650–900 °C) the data derived from the work of Mei *et al.* have been used and at high temperatures (1000–1200 °C) the Ga self-diffusion data have been employed. If only the interdiffusion data are used then large discrepancies between the independent sets of data can be seen (Fig. 2). At some temperatures (for example 850 °C), there are approximately three orders of magnitude variation in the value of the interdiffusion coefficient obtained. It follows that data at higher and lower temperatures are needed to obtain a more reliable value for the activation energy. Tan and Gösele later remarked [12] that the agreement between the self-diffusion data and the interdiffusion data was probably coincidental.

The picture has not become clearer with the passing of time. It is now known that the type of capping layer used in thermal annealing experiments critically affects the interdiffusion of the layers. Moreover, the ambient arsenic overpressure additionally affects the interdiffusion. (This explains some of the discrepancies highlighted in Fig. 2. The dots indicate results obtained with an SiN_x cap, whilst the open squares and open triangles represent data obtained with no cap and a SiO_2 cap, respectively).

Guido *et al.* [13] showed that the interdiffusion coefficient underneath an SiN_x capping layer was significantly less, by almost an order of magnitude, than that underneath a SiO_2 cap. Moreover, they observed that the interdiffusion coefficient of the uncapped samples, derived from their photoluminescence results, varied with the arsenic vapour pressure over the sample. This effect is clearly seen in Fig. 3. The increase in the interdiffusion coefficient with arsenic pressure at high arsenic pressures was assigned to the diffusion of V_{Ga} from the surface, whereas the increase in the interdiffusion coefficient with decreasing arsenic overpressure at low arsenic pressures was assigned to the increase in I_{Ga} concentration at the surface. This observation was confirmed by Furuya *et al.* [14] who also observed that the photoluminescence efficiency decreased with increasing arsenic overpressure.

If the explanation of the above effect is correct then the interdiffusion coefficient should be depth-dependent. Indeed this has been found to be the case [15, 16]. The depth dependency is clearly illustrated in Fig. 4a which shows the effect of annealing, for 3 h at 1000 °C, a superlattice structure consisting of 20 layers of GaAs, 50 nm thick, sandwiched between 21 layers of AlAs, also 50 nm thick. The topmost layers of the structure are intermixed whilst those deeper in the crystal show little or no intermixing. Fig. 4b shows a piece of the same wafer annealed at the arsenic dissociation pressure for the same period of time. In this case the intermixing is uniform and there is very little interdiffusion of the layers. These results seem to be in conflict with the findings of Guido *et al.* [13] and Furuya *et al.* [14]. This discrepancy could be caused by the two different methods used to assess the intermixing of the layers. Baba-Ali *et al.* [16] used an optical microscope to visually inspect bevelled sections and in addition they performed their experiments with relatively thick layers, whereas Guido *et al.* [15] used photoluminescence which necessitated a narrow single quantum well. Perhaps more importantly, the two sets of experiments were performed with significantly different annealing conditions. Guido *et al.*'s experiments were undertaken at 825 °C for 25 h whilst those of Baba-Ali *et al.* were carried out at 1000 °C for 3 h.

To confuse the situation further, Guido *et al.* [15] have more recently investigated the interdiffusion of a lightly p-doped quantum well. It was found that the interdiffusion of the well was independent of the arsenic overpressure. Moreover, Baba-Ali *et al.* [16] predicted the amount of interdiffusion from Equation 1 and found that it was significantly more than the observed intermixing in the deepest parts of either Fig. 4a or Fig. 4b. This is not surprising since the types of capping layer, depth and grown-in vacancies will all affect the interdiffusion coefficient. The allocation of

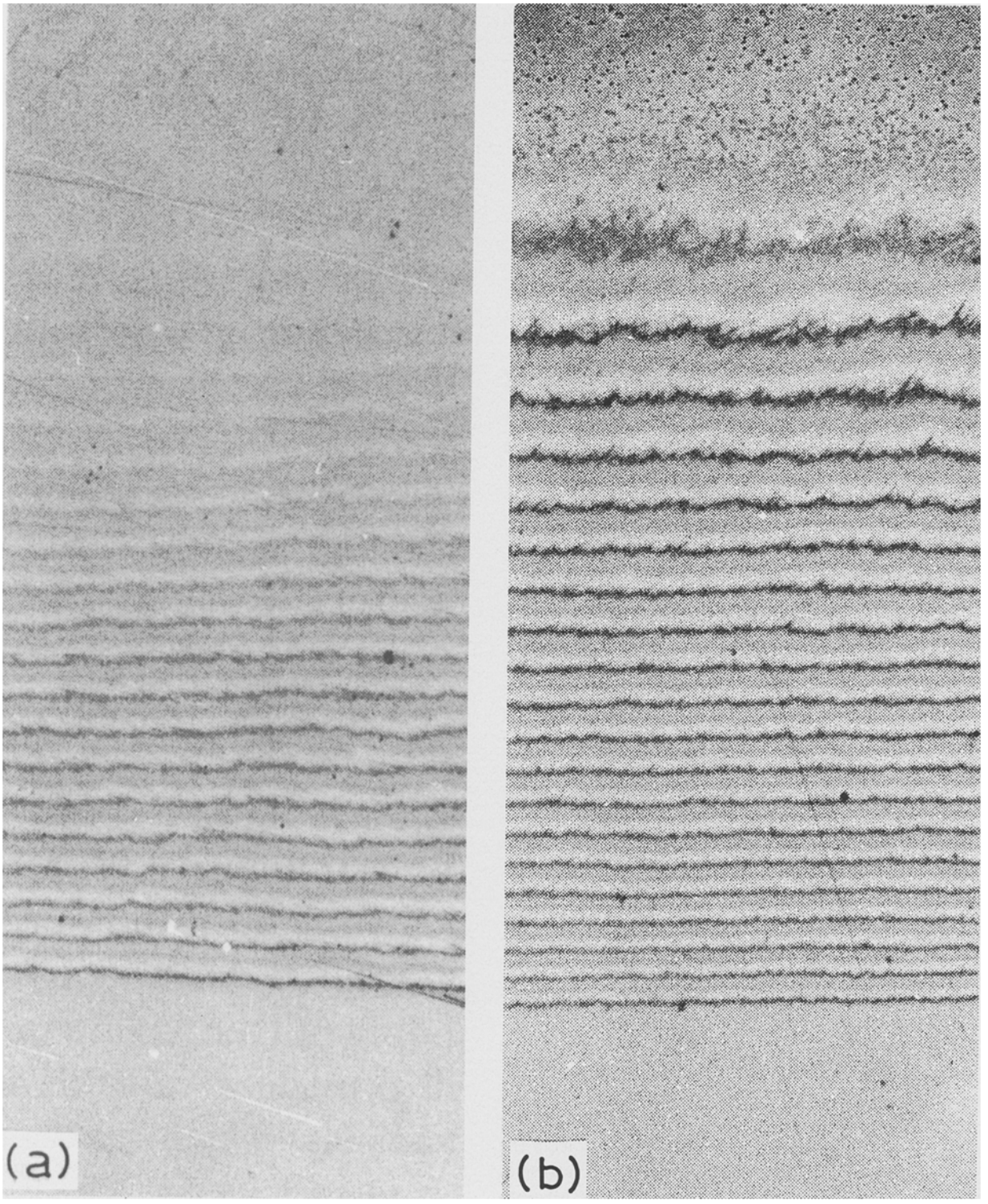

Figure 4 Effect of annealing a superlattice structure for 3 h at 1000 °C with an As overpressures of (a) 0.4 atm and (b) dissociation pressure (after Baba-Ali *et al.* [16]).

one constant value for the interdiffusion coefficient is therefore flawed.

Recently several authors [18–21] have suggested that at a particular temperature there is a range of interdiffusion coefficients. The phase diagram of GaAs shows that GaAs exists over a range of stoichiometry, that is over a range of equilibrium values of V_{Ga}, V_{As}, I_{Ga} and I_{As}. Since one or more of these point defects are responsible for the interdiffusion of GaAs and GaAlAs, it is therefore not unreasonable to assume that the interdiffusion coefficient will also have a range of values depending on the crystal stoichiometry.

The variation of the measured interdiffusion coefficient with arsenic overpressure leads to the conclusion that two point defects are responsible for the intrinsic interdiffusion in GaAs–GaAlAs. The proposed defects are V_{Ga}^{3-} and I_{Ga}^{2+} (in general it is the group III vacancy and interstitial). Moreover, Tan *et al.* [21] have derived expressions for the interdiffusion coefficient via both point defects when there is 1 atm of arsenic

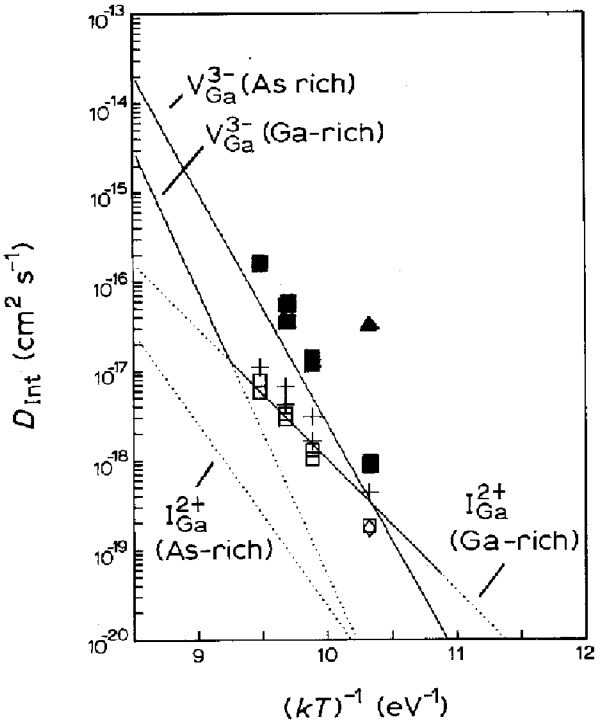

Figure 5 Arrhenius plot of the interdiffusion coefficient under Ga-rich conditions and under 1 atm As overpressure. The dotted lines represent the components of the interdiffusion caused by group III interstitials and group III vacancies. The dominant mechanism is represented by a full line. Experimental data points [17, 22] are also shown: (■, ▲) obtained under As overpressure; (+) under dissociation pressure; (□, ◇) under gallium-rich conditions; (■, +, □) data of Hsieh *et al.* [17]; (◇, ▲) data of Olmsted and Houde-Walter [22].

overpressure and when the surface is gallium-rich. These are plotted in Fig. 5. It can be seen from this diagram that under As-rich conditions (1 atm of arsenic overpressure) the dominant interdiffusion mechanism is V_{Ga}^{3-}. However, under Ga-rich conditions the interdiffusion, at low temperatures, occurs via I_{Ga}^{2+} changing over to V_{Ga}^{3-} at around 1000 °C. The work of Tan *et al.* [21] is in agreement with the experimental results of Hsieh *et al.* [17] but not with the arsenic-rich results of Olmsted and Houde-Walter [22]. The theory predicts that the intermixing for samples which had a gallium-rich surface should have smaller interdiffusion coefficients than those samples which were annealed under 1 atm of As_4. This is observed experimentally in both sets of results (Fig. 5). The discrepancy between the measured values and the theoretical ones is not acceptable to a device engineer who may wish to model the interdiffusion process so that a good estimate for the annealing conditions can be made. Before moving on, it should be noted that the use of different capping layers to achieve different levels of intermixing has been successfully applied to the manufacture of optoelectronic devices [23, 24].

2.2. InGaAs–InAlAs

In the lattice-matched InGaAs–InAlAs system one only expects an interchange of gallium and aluminium atoms since the In concentration is approximately constant. In addition, the system should remain approximately lattice-matched even when there is an interchange of gallium and aluminium atoms. Seo *et al.* [32] observed the intermixing of the InGaAs barriers and InAlAs wells by photoluminescence. The energy shift of the photoluminescence line arising from the well was towards higher energy, indicating that interdiffusion of the gallium and the aluminium atoms was occurring. The interdiffusion coefficients obtained from their results were several orders of magnitude greater than those obtained for the AlAs GaAs system. This can be seen clearly in Table I which compares the interdiffusion coefficients of the InGaAs–InAlAs system and the GaAs–GaAlAs system. However, the actual values obtained should be treated with caution since the interdiffusion coefficient obtained varied with time, indicating that the model they used to derive the interdiffusion coefficient is invalid. The interdiffusion of InGaAs–InAlAs therefore cannot be described by a single diffusion coefficient. This may be due to two reasons: the interdiffusion coefficient may depend on the concentration of the aluminium (as in AlGaAs–GaAs) or a defect may be diffusing from the surface causing the interdiffusion coefficient to vary with time. In the latter explanation the most probable defect will be a group III vacancy.

TABLE I Comparison of interdiffusion coefficients for the InGaAs–InAlAs and GaAs–AlGaAs systems. The range of interdiffusion coefficients for the GaAs–AlGaAs system is taken from Fig. 2 whilst the interdiffusion data for the InGaAs–InAlAs system are taken from Seo *et al.* [32]

	D_{int} (cm^2 s^{-1})	
Temperature (°C)	InGaAs–InAlAs	GaAs–AlGaAs
750	3×10^{-16}	$\sim 10^{-19}$
800	1.1×10^{-15}	10^{-19}–10^{-18}
850	3.0×10^{-15}	10^{-19}–10^{-16}

To confuse the situation there have been several reports of indium diffusing into the barriers. This effect was first observed by Baird *et al.* [33] who annealed a single 100 nm layer of InGaAs sandwiched between two layers of InAlAs. Their results are shown in Fig. 6. This shows an increase in the indium signal on the InGaAs side of the two interfaces. This effect was explained in terms of the different diffusivities of the gallium and aluminium and the need for the sample to maintain III–V stoichiometry. In samples which have been studied by photoluminescence one would expect this effect to manifest itself as a red shift in the photoluminescence line. This has been observed in $In_{0.53}Ga_{0.27}Al_{0.20}As$–$In_{0.53}Ga_{0.47}As$ multi-quantum well structures [34]. There is at present no satisfactory explanation why sometimes one sees a blue shift (gallium–aluminium interdiffusing) in the photoluminescence peak and at other times a red shift (gallium and indium interdiffusing). The most likely explanation is the effect of residual stress, and stress caused by different masks.

A high-resolution electron microscopy study of the interdiffusion of InGaAs–InAlAs superlattices latticed

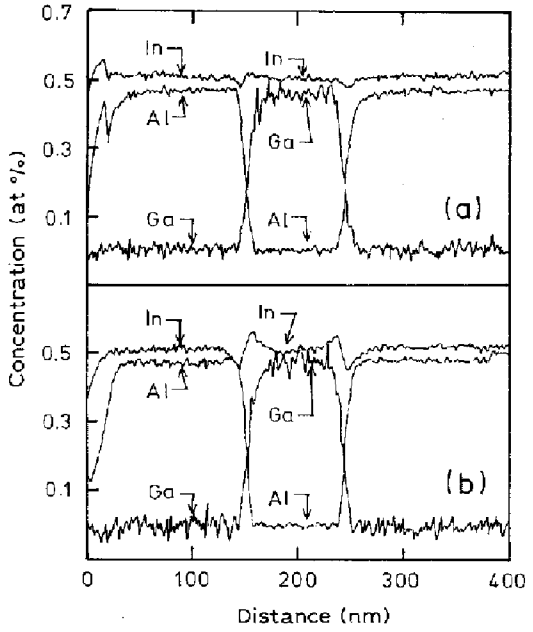

Figure 6 Auger profile through a 100 nm InGaAs layer surrounded by InAlAs which shows the increase in the In content of the InGaAs layer following a 812 °C 10 h anneal: (a) profile of material as grown, (b) profile after thermal anneal performed in flowing nitrogen (after Baird *et al.* [33]). (Reproduced with the permission of the American Institute of Physics.)

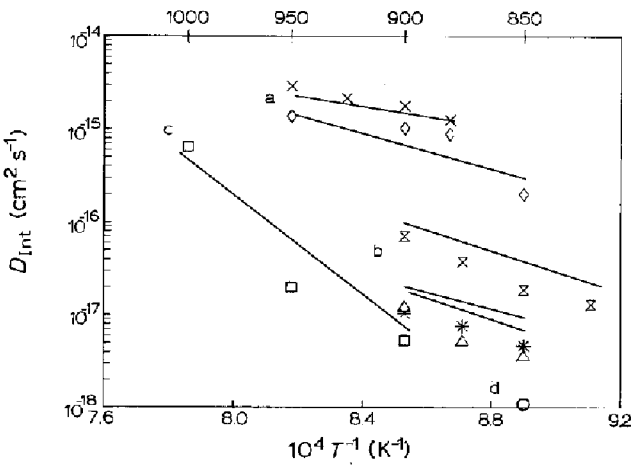

Figure 7 Arrhenius plot of the interdiffusion coefficient for InGaAs–GaAs. The data marked (a) are from the work of Kothiyal and Bhattacharya [40] whilst those marked (b) are from Hsieh *et al.* [43] and (c) from Gillin *et al.* [41]. (○) MQW ($x = 0.15$), (*) SQW ($x = 0.15$), (□) MQW ($x = 0.14$), (◇) MQW ($x = 0.20$), (×) SQW ($x = 0.24$), (△) SQW ($x = 0.15$) + Ga, (⊠) SQW ($x = 0.15$) + As.

matched to InP has been performed by Mallard *et al.* [35]. They estimated the amount of interdiffusion from looking at the micrographs obtained under (200) diffraction conditions and by energy-dispersive X-ray analysis. They also observed out-diffusion of the indium from the InAlAs barriers into the InGaAs well. This was also coupled with the asymetrical diffusion of the gallium and aluminium. These results seem to provide further evidence for the explanation given by Baird *et al.* [33].

It should be reiterated that the explanation of Baird *et al.* does not explain why one sometimes observes a red shift and others a blue shift. It does, however, explain why one could obtain a red shift.

The effect of capping the InGaAs–InAlAs with different materials has been investigated. Both SiN_x [36] and SiO_2 have been used [37, 38]. Initial results of Chi *et al.* [37] indicated that there was less intermixing under an SiO_2 cap than in the areas which were not capped. However, in later studies the opposite was observed [38]. The SiO_2 films used in these two experiments were deposited in slightly different ways. In the first, the SiO_2 was deposited by r.f. sputtering whilst in the second it was deposited by electron beam evaporation. In addition different annealing conditions were used. Further investigation by secondary ion mass spectroscopy (SIMS) of the interdiffusion under the electron beam-deposited SiO_2 found that there was a significant amount of silicon and oxygen diffusion. It was therefore postulated that the intermixing was due to the diffusion of the silicon rather than solely to the heat treatment.

For SiN_x capping, after one rapid thermal anneal for 15 s at 850 °C, the intermixing under the SiN_x cap was approximately the same as in the uncapped region. On the other hand when three 5 s anneals were performed instead of the one 15 s anneal a difference in the photon energy of the photoluminescence coming from the capped and uncapped regions was observed [36].

2.3. InGaAs–GaAs

The interdiffusion of strained InGaAs–GaAs has been investigated by several groups [39–43]. The data obtained by these workers are shown in Fig. 7. Apart from the work of Joncour *et al.* [39] the interdiffusion coefficient derived was obtained by photoluminescence. Joncour *et al.* used X-ray diffraction but, as in the photoluminescence measurements, they used a concentration-independent interdiffusion coefficient. They did remark, however, that as time proceeded, the interdiffusion coefficient obtained varied from 0.8×10^{-18} to 2.0×10^{-18} cm^2 s^{-1}. Kothiyal and Bhattacharya [40] annealed two $In_xGa_{1-x}As$–GaAs multi-quantum well structures each with a different indium content. They found that the interdiffusion coefficients they obtained for each of the quantum wells were different. They noted that the value of the interdiffusion coefficient they obtained was significantly greater than the values published by Joncour *et al.* [39]. They explain the differences in the values obtained in terms of the different times involved. The early work of Joncour *et al.* used diffusion times of 17–71 h at 850 °C whilst Kothiyal and Bhattacharya [40] used times between 5 and 25 s. Kothiyal and Bhattacharya argued that in the early stages of annealing the interdiffusion coefficient is higher owing to the higher concentration of point defects. However, as the diffusion time and temperature increase the defects are annealed, which reduces the interdiffusion coefficient. If this explanation is correct then the validity of their single diffusion coefficient should again be questioned. They also suggested that the effects of differing amounts of strain could also have caused some discrepancy between the two sets of results. This is borne out by Fig. 7. The samples which have the highest

amounts of strain may also have a larger number of dislocations. Dislocations can act as sources of point defects and so the samples with the largest density of dislocations (the heavily strained ones) will have a larger interdiffusion coefficient. From Fig. 7 it can be seen that apart from the work of Gillin *et al.* [41] the activation energies of the interdiffusion processes seem to be approximately the same. It should be noted, however, that the work of Gillin *et al.* differed in two significant ways: the sample was capped with SiN_x and the sample was continually cycled. Although not strictly valid for InGaAs–GaAs since a different system was used (InGaAs–InAlAs), the work of Miyazawa *et al.* [36] shows that cycling a sample through several shorter anneals produces a larger shift in the photoluminescence line than when one single anneal is used. If this effect is not taken into account, then an overestimate of the interdiffusion coefficient will be obtained. Moreover, one would expect this effect to be larger at higher temperatures and so the measured activation energy will be greater than the actual one. It should be noted, however, the work of Miyazawa *et al.* [36] used very short annealing times coupled with slow temperature ramps, whilst that of Gillin *et al.* [41] used much longer anneal times and a much faster ramp.

The work of Hsieh *et al.* [43] has shown that the interdiffusion of a single InGaAs well depends on the arsenic overpressure. Their results, which are included in Fig. 7, indicate that the group III vacancy is playing an important role. They also demonstrated that larger photoluminescence shifts were observed if an AlGaAs cladding layer was used. They attributed this increase of the photoluminescence shift to the diffusion of aluminium from the cladding layers into the barrier. In addition they confirmed that the interdiffusion rate depends on the indium content.

The effects of an SiO_2 mask on the interdiffusion of an AlGaAs-clad InGaAs–GaAs quantum well has been investigated by Major *et al.* [42]. They found that aluminium has a high solubility in SiO_2 which causes some of the silicon and oxygen to diffuse into the sample. In all probability the aluminium reduces the SiO_2 according to the chemical reaction

$$4Al + 3SiO_2 \rightarrow 2Al_2O_3 + 3Si$$

They showed that the silicon concentration in the surface layers of the AlGaAs and the amount of aluminium in the SiO_2 both increased with the arsenic overpressure. However, the intermixing of the InGaAs well did not follow this trend. Three experiments were performed with differing amounts of arsenic in the diffusion ampoule. In the first experiment no arsenic was added to the ampoule, whilst in the second and third 10 and 30 mg of arsenic was added, respectively. A large amount of indium diffusion was only observed in the sample annealed with 10 mg of arsenic. This correlated with the silicon penetration depth. Under the SiN_x mask a much smaller shift in the photoluminescence line associated with the well was observed. This allowed the fabrication of lasers using SiN_x and SiO_2 masks.

2.4. InGaAs–InP

Interdiffusion in the InGaAs–InP system has been studied by Temkin *et al.* [44] who found that, during a thermal anneal, the photoluminescence peak shifted to higher energies, which is consistent with the interdiffusion of the InGaAs and InP. However, transmission electron microscopy (TEM) pictures indicated that the interface between the barrier and the wells was still abrupt and, moreover, the thickness of the wells was seen to have increased. Temkin *et al.* suggested that the system remains lattice-matched during the anneal. More recently, X-ray rocking curve measurements and Raman spectroscopy of annealed InGaAs InGaAsP multi-quantum well structures have shown that the system does remain lattice-matched during the thermal anneal [45, 46]. However, the later studies found that there was a smearing of the interface which is opposite to the observations of Temkin *et al.* [44] but in agreement with the photoluminescence study performed by Fujii *et al.* [47]. This is in contrast with the experiments of Nakashima *et al.* [48] who found that the interface between the wells and the barrier was sharp but no longer latticed-matched. It should be noted, however, that the experiment of Nakashima *et al.* used SiO_2 to prevent surface degradation during the thermal anneal whereas the others used either phospine overpressure or Si_3N_4.

To explain the observations [44 47], the explanation provided by Fujii *et al.* [47] will be invoked. The diffusion of the phosphorus atoms in the barrier and wells is given by Fick's law. The first equation below represents the diffusion of the phosphorus in the barrier and the second that in the well.

$$\frac{\delta C_b}{\delta t} = D_b \frac{\delta^2 C_b}{\delta X^2} \qquad (2)$$

$$\frac{\delta C_w}{\delta t} = D_w \frac{\delta^2 C_w}{\delta X^2}$$

C_b and C_w are the phosphorus concentrations in the barrier and the well, respectively. The diffusion coefficients in the barrier and well are assumed to be different and are given the symbols D_b and D_w. In order to solve these equations it is necessary to define mathematically the flux (j_h) of phosphorus atoms crossing the boundary between the barrier and the well. The form chosen by Fujii *et al.* [47] was

$$j_h = D_h(C_{b_0} - C_{w_0}) \qquad (3)$$

C_{b_0}, C_{w_0} and D_h are the concentration of the phosphorus on the barrier and well side of the interface and a constant of proportionality, respectively. Fujii *et al.* [47] found that their experimental results suggested that D_h was small in relation to D_b and D_w, which indicates that interdiffusion is limited by the diffusion of phosphorus across the interface. This was explained in terms of the addition potential energy, owing to the increase in strain, when an arsenic atom diffuses from the well into the barrier or a phosphorus atom from the barrier into the well. Although this analysis is not mathematically rigorous, since it ignores the diffusion of the group III elements, it does provide a plausible

explanation for the observations. Moreover, the work of Temkin *et al.* [44] can also be explained. The relatively slow diffusion of the group V elements across the interface compared to their diffusion within either barrier or well means that the interface remains sharp, and so in the TEM pictures presented by Temkin *et al.* one would expect to observe very little degradation of the interface sharpness.

2.5. GaAsSb–GaAs

This strained layer system has been studied by Gillin *et al.* [49]. Like all the other systems described, there are very few data for self-diffusion in GaSb and none for the ternary system [50]. The results of Gillin *et al.* are very interesting since they show that the interdiffusion of GaAs–GaAsSb cannot be described by Fick's law. Another observation which is very interesting is the effect of grown-in dopants on the stability of the layers. Both silicon and beryllium slow down the interdiffusion process. This observation is in complete contrast with the other III–V systems such as GaAs–GaAlAs where the dopant causes a dramatic increase in the interdiffusion.

3. Zinc

3.1. GaAs–AlAs

The diffusion of zinc into GaAs is generally accepted to be interstitial in nature, the interstitial zinc being positively charged. There are, however, two mechanisms for the incorporation of zinc on to the lattice. In the first the zinc moves on to a vacant gallium site [51] and in the second the zinc "kicks" off a group III atom from its lattice site [52]. It then moves on to the now-vacant lattice site. These two mechanisms can be represented by the quasi-chemical reactions

$$Zn_i^- + V_{Ga} \rightleftharpoons Zn_s^- + 2h^+$$

$$Zn_i^+ + Ga \rightleftharpoons Zn_s^- + I_{Ga} + 2h^+$$

In the first case, there will be an undersaturation of gallium vacancies caused by the zinc moving on to the substitutional site. One possible mechanism for the crystal to recover its equilibrium value for gallium vacancies is via Frenkel pair generation [53]

$$Ga \rightleftharpoons I_{Ga} + V_{Ga}$$

If the rate of generation of Frenkel defects is faster than the zinc diffusion rate then it could be argued that the two mechanisms are equivalent. If a zinc diffusion is performed at temperatures above approximately 750 °C, dislocation loops are observed [54]. The nature of these dislocation loops has been analysed by Ball *et al.* [55] who found them to be interstitial in nature. To explain the generation of these loops the kick-out mechanism is used. As the interstitial zinc moves on to the lattice site there will be an increase in the concentration of interstitial gallium. If this concentration rises above a critical concentration, it is energetically favourable for the interstitials to form dislocation loops. Moreover, the dissociative mechanism could also have been used to explain the presence of these loops so long as the additional step of Frenkel pair generation is included. The diffusion of zinc into AlGaAs and AlAs has not been extensively studied and the work is mainly limited to the measurement of diffusion depths [56–60]. This work has found that the diffusion rate in GaAlAs increases as the aluminium content increases. It is also not unreasonable to assume that the diffusion mechanism for zinc in the ternary GaAlAs is the same as in GaAs.

The original article [2] which reported the effect of diffusing zinc on the stability of the GaAs–GaAlAs superlattices layers suggested a variation of the dissociative mechanism. Rather than the interstitial zinc immediately jumping on to a vacant group III site, a intermediate vacancy–interstitial zinc complex formed. It was suggested that this complex could then take part in the self-diffusion process.

Later van Vechten [61] suggested two more detailed mechanisms based on the Jain diffusion mechanism for phosphorus into GaAs [62]. Both of these mechanisms involved the movement of atoms around a hexagonal ring on the (1 1 1) planes and involved both anti-site defects and vacancies. In these mechanisms all defects were assumed to be charged. Group III and group V vacancies were assumed to be singly charged. The group III vacancy charge was negative whereas the group V vacancy charge was assumed to be positive. Anti-site defects were assumed to be doubly charged, with a group III atom on the group V lattice site negative, and a group V atom on a group III site positive. If there is a group V vacancy in the ring then a group III atom can easily move on to this site, creating an anti-site defect and a group III atom (Fig. 8). The ring will now have a total charge of -3 and this will cause a Coulombic attraction between the interstitial zinc and the defect cluster, reducing the energy of the defect cluster. (Note that the charge on the interstitial zinc has changed so that it is positively doubly charged). In the next step, a group V atom moves on to the group III site creating an additional anti-site defect and a group V vacancy. The total charge is $+1$ and the zinc atom is no longer needed to reduce the energy and drifts away. As can be seen the process leaves a trial of anti-site defects. However, after twelve similar steps it can be shown that the number of anti-site defects in the ring reduces to zero. More importantly, this movement of atoms around the ring will enhance the self-diffusion of both group III and group V elements and the ratio of enhancement of the group III to the group V atoms is 3:2. In the second mechanism, a divacancy rather than a single vacancy was assumed to be the defect responsible for the movement of the atoms. van Vechten [61] demonstrated that fewer anti-site defects would be generated. Referring to Fig. 9, as in the first ring mechanism, the first movement of atoms generates an anti-site defect, which is removed after the second step. In the absence of zinc interstitials, this ring mechanism would move equal numbers of group III and group V atoms. However, the Coulombic attraction between the zinc atom and the negatively charged group III anti-site defect would enhance the vacancy diffusion of

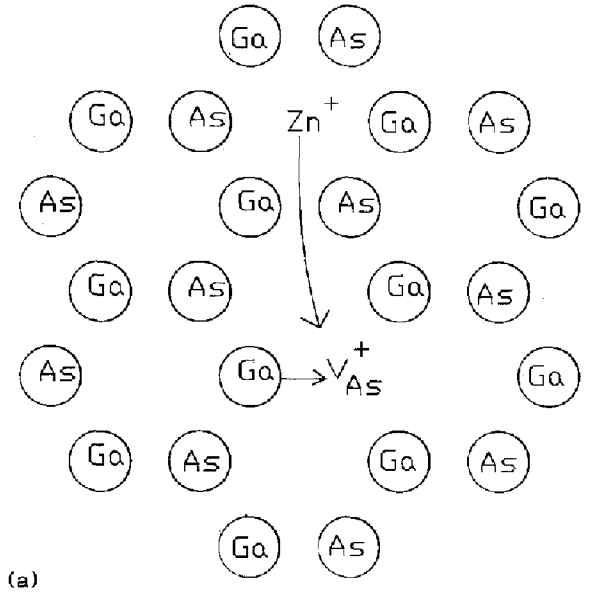

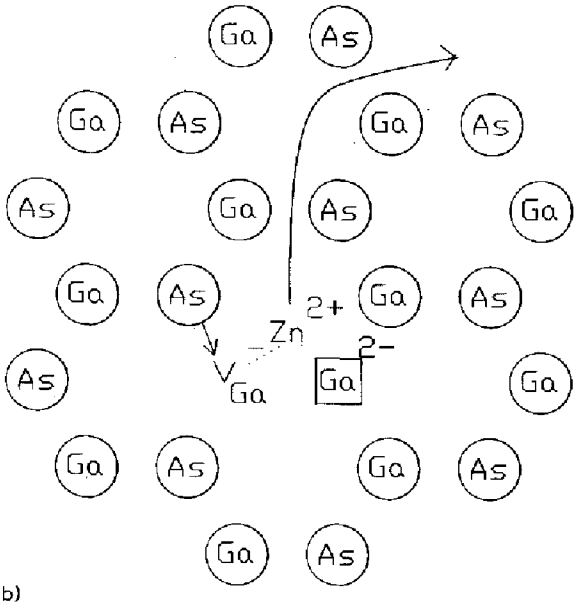

Figure 8 The first three steps of the first van Vechten intermixing mechanism for zinc-induced disordering in GaAs–AlAs superlattices. Anti-site defects are shown as squares (after van Vechten [61]).

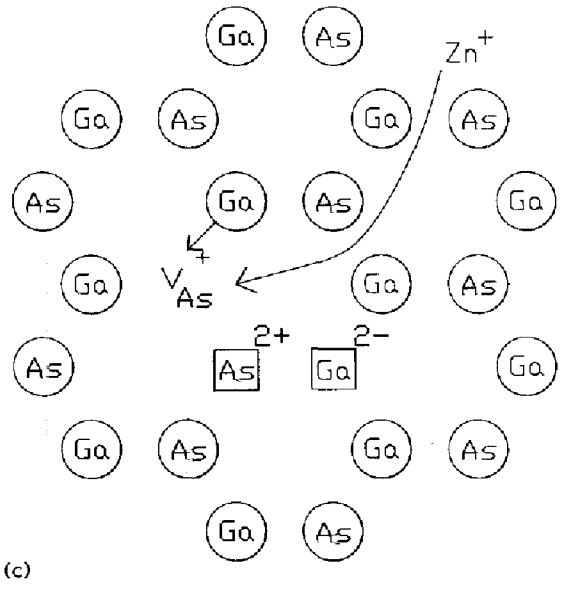

the group III atoms (so the steps shown in Fig. 9 are strongly favoured in the presence of zinc). This mechanism would therefore appear to predict intermixing of the group III sites but not the group V sites.

More recently [11], an interstitial mechanism has been proposed. As stated above, a consequence of diffusing zinc is the generation of group III interstitials. Since these interstitials are not bound to a lattice site, the diffusion of the interstitials is expected to be fast. It is proposed that these interstitials are responsible for the enhancement of the interdiffusion.

A detailed investigation of zinc-induced disordering has been performed by Harrison *et al.* [1, 63] who used both SIMS and TEM. This work showed that as a result of the zinc diffusion at 700 °C, dislocation loops were formed in the AlAs layers. The loops can be seen in Fig. 10 which shows a TEM micrograph of a 3.5 min 700 °C zinc diffusion. The same sample has been investigated by SIMS and this is shown in Fig. 11a. From these two figures it can be seen that the position of the dislocation loops is slightly deeper than the disordering, but within the zinc-diffused areas. The oscillations in the zinc concentration seen in the SIMS have been assigned to differences in solubility of the zinc in GaAlAs and GaAs. The solubility of zinc in $Ga_{1-x}Al_xAs$ decreases with increasing aluminium content x. This effect is most striking in the 15 min 700 °C zinc diffusion, which totally disorders the 2 μm superlattice. The SIMS result for this sample is shown in Fig. 11b and it can be seen that the zinc signal increases when one moves away from the disordered superlattice region which is marked A. Boltaks *et al.* [64] measured the surface concentration of zinc-diffused $Al_xGa_{1-x}As$ as a function of x, the aluminium content. They found that it decreased with increasing aluminium content. Therefore the above results on zinc-induced disordering of GaAs–AlAs superlattices are in agreement with the findings of Boltaks *et al.* [64].

The generation of the dislocation loops provides evidence for the excess-interstitials mechanism. As the zinc diffuses, it generates group III interstitials by the mechanism described earlier. The concentration of interstitial group III atoms within the crystal will be greatly enhanced [65]. If these diffuse through the crystal and in turn become substitutional by kicking out another group III atom from its lattice site, then there will be a significant increase in the interdiffusion. For example, in one of the GaAs layers of a superlattice the zinc will create a gallium interstitial when it moves on to the substitutional site. This interstitial will be able to diffuse quickly through the crystal, reaching a layer of AlGaAs, where there is a significant probability that it will "kickout" an aluminium atom, thereby increasing the gallium content. In a similar way, aluminium interstitials will be generated in an AlGaAs layer and will diffuse to the GaAs layers. If the increase in concentration of the group III interstitials is sufficiently high, oversaturation occurs and it may be energetically favourable for the crystal to form dislocation planes.

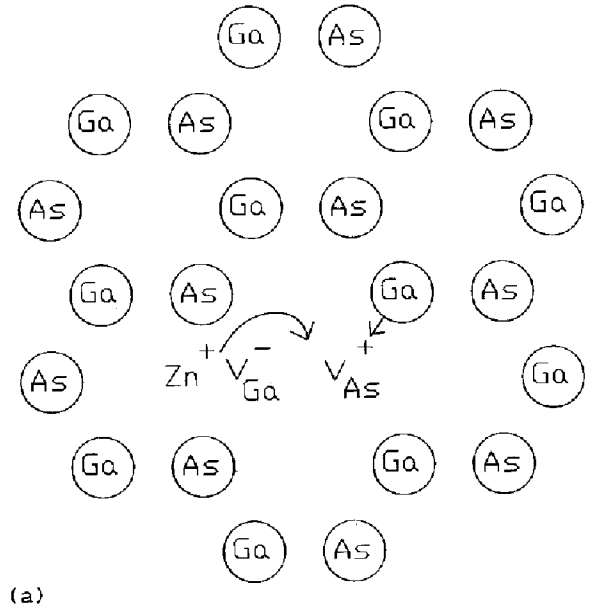

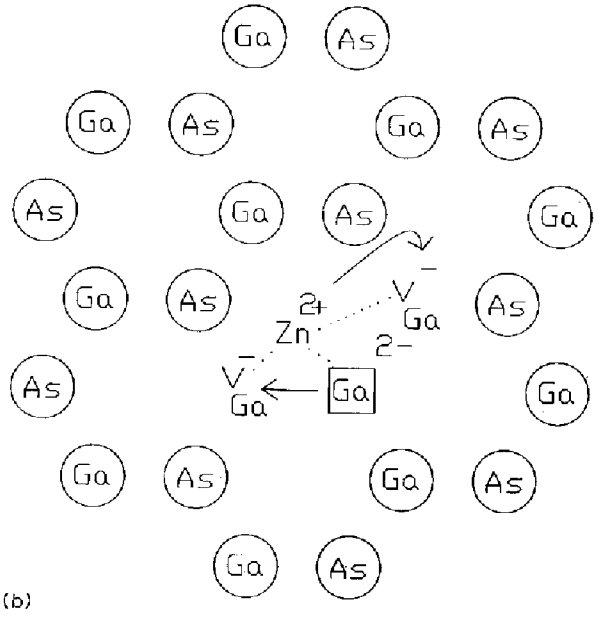

Figure 9 The first three steps of the second van Vechten mechanism. Anti-site defects are shown as squares (after van Vechten [61]).

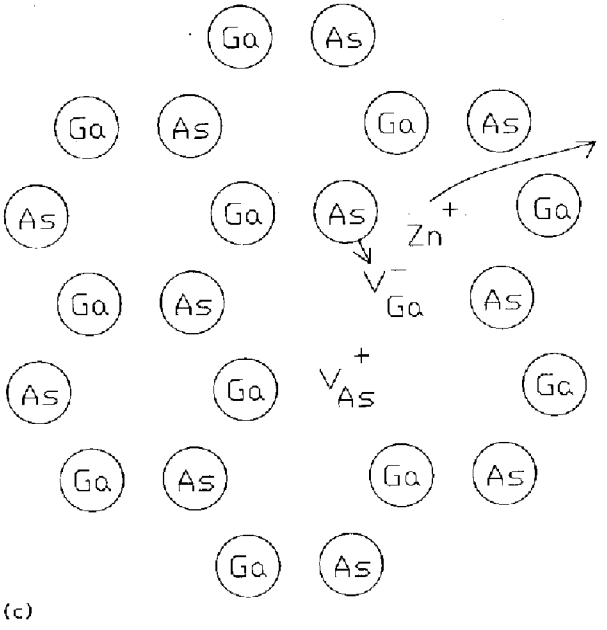

Tab and Gösele [12] noted that the enhancement of the interdiffusion caused by the diffusion of zinc was confined to the zinc-diffused region and that the size of the enhancement was very large. They suggested that the group III interstitials which are responsible for the interdiffusion effect are positively charged. The p-type doping of the zinc would then increase the population of this species, thereby increasing the interdiffusion. They noted that an oversaturation of group III interstitials was also necessary. It should be emphasized, however, that the region with the greatest group III interstitial concentration is slightly behind the diffusion front [1]. The evidence for this comes from the position of the dislocation loops which are slightly behind the diffusion front. It is expected that the disordering of the GaAs–AlAs layers will be greatest in the regions of high group III interstitial concentration, i.e. in the region between the diffusion front and the surface, which could explain why zinc-induced disordering is only confined to the zinc-diffused region.

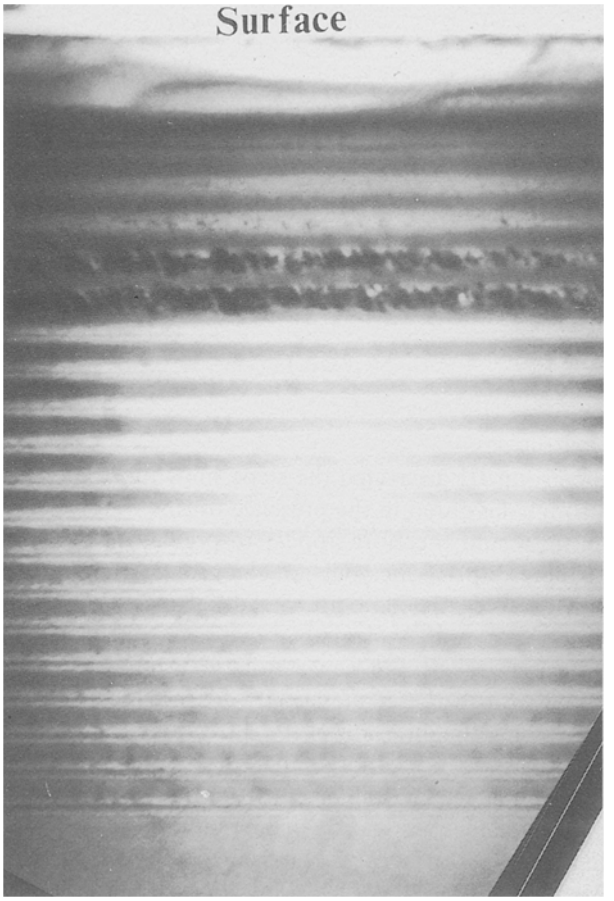

Figure 10 Cross-sectional transmission electron micrograph of a GaAs–AlAs superlattice which shows the dislocation loops generated in the AlAs by the diffusion of zinc. The diffusion was performed for 3.5 min at 700 °C.

3.2. InGaAs–InAlAs

The diffusion of zinc into InGaAs–InAlAs has been studied by several workers [66, 67] and has been shown to intermix the gallium and the aluminium.

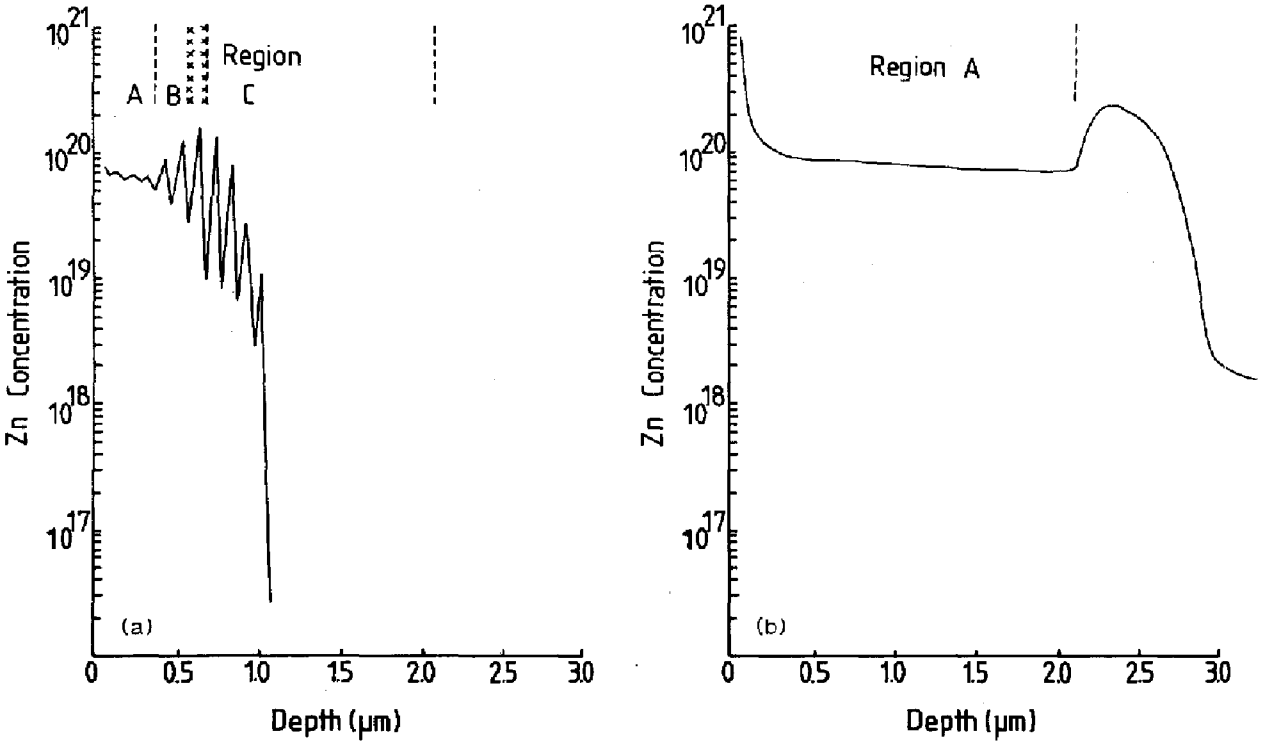

Figure 11 SIMS profiles for zinc-diffused GaAs–AlAs superlattices after (a) 3.5 min and (b) 15 min at 700 °C. The crosses in (a) locate the position of the dislocation loops observed in the TEM. (Reproduced with the permission of the American Institute of Physics.)

This system is lattice-matched over a variety of compositions and therefore may be suitable for the manufacture of IID devices. The mechanism causing the enhancement of the intermixing in this system is believed to be similar to that operating in GaAs–GaAlAs.

3.3. GaAs–GaAsP

The diffusion profiles of zinc in GaP [68] are very similar to those obtained in GaAs, which indicates that the diffusion mechanism is similar to that of zinc into GaAs. Data from the isoconcentration radioactive tracer experiments of Chang and Pearson [69] indicate that the diffusion coefficient of zinc in GaP depends on the square of the zinc concentration, which is the same dependence as that observed in GaAs. The diffusion of zinc into GaP does however strongly depend on the surface conditions [70].

In the experiments of Camras *et al.* [71] zinc was diffused at 825 °C for 14 h into a $GaP_{0.6}As_{0.4}$–GaAs strained superlattice. In this series of experiments, enhancement of the interdiffusion of the group V elements was observed. This result is very interesting in the light of the work described above which was performed on AlGaAs–GaAs superlattices. If a similar zinc diffusion process is assumed then the explanation given for the AlGaAs–GaAs superlattices does not explain the intermixing of the $GaP_{0.6}As_{0.4}$–GaAs superlattices. There is however one important difference between the two systems, and that is the presence of strain in the $GaP_{0.6}As_{0.4}$–GaAs superlattice. During the thermal annealing of the superlattice, misfit dislocations may occur causing the generation of point defects. The interaction between these defects and the diffusing zinc may cause the impurity-induced disordering effect.

3.4. InGaAsP–GaAs

There have been several reports of diffusion into strained InGaAsP–GaAs multi-quantum wells [72, 73]. Park *et al.* [72] diffused zinc at 700 °C for 25 h into an $In_{0.06}Ga_{0.94}P_{0.05}As_{0.95}$ layer grown by LPE on a GaAs substrate. By observing the diffusion of the phosphorus and indium into the GaAs substrate they could analyse the effect of the zinc diffusion. The mole fractions of the indium and phosphorus were kept deliberately low so as to minimize the effect of strain. They found that the diffusion of zinc enhanced both indium and phosphorus interdiffusion. However, the indium diffused much faster than the phosphorus, by approximately two orders of magnitude. To obtain a diffusion constant for the indium they analysed the indium profile by the Boltzmann–Mantano method. The diffusion coefficient they obtained was independent of the indium concentration and was equal to 5×10^{-14} cm^2 s^{-1}. They then proceeded to obtain a value of 6×10^{-16} cm^2 s^{-1} for the phosphorus diffusion. The Boltzmann–Mantano method assumes that the diffusion constant depends on the concentration only and is not a function of time. Since in the above experiment the enhancement does not occur until the zinc reaches the interface, the indium and phosphorus diffusion coefficients will also be functions of time and so the Boltzmann–Mantano analysis will be invalid. Therefore the values obtained by Park *et al.* [72] for the indium and phosphorus diffusion coefficients should be treated with caution.

Park *et al.* explained the enhancement of the indium diffusion in terms of the interstitial-substitutional

mechanism used to explain zinc intermixing in AlGaAs–GaAs superlattices. However, the enhancement of the group V interdiffusion rate does not fit neatly into this mechanism. Park *et al.* gave no reason for the small enhancement of the phosphorus diffusion coefficient.

Deppe *et al.* [73] have diffused zinc into an $In_{0.5}(Al_{0.4}Ga_{0.6})_{0.5}P$–GaAs heterostructure for 20 h at 600 °C. In this series of experiments the heterostructures contain both indium and phosphorus and therefore one would expect a build-up of strain at the interface once interdiffusion takes place. The results indicate again that zinc enhances the diffusion of the group III atoms, which was explained once again by the interstitial-substitutional mechanism. However, Deppe *et al.* did not observe any enhancement in the diffusion of the group V elements. It should be realised that the previous results which have demonstrated group V enhancement have been performed under diffusion conditions more severe than those used in Deppe *et al.*'s experiment. It is therefore possible that in Deppe *et al.*'s experiment enhancement of the group V diffusion has occurred but it is too small to observe. A second point should be noted: in the SIMS profile through the heterostructure, the indium signal dips at the interface. This may be an artefact of the SIMS process or it may be real, indicating that strain at the heterostructure interface has had an effect on the interdiffusion process.

3.5. InGaAsP–InP

The diffusion mechanism of zinc into InP differs from that of GaAs. The electrically active concentration of zinc-diffused InP is significantly less than the atomic concentration of the zinc, which suggests that the majority of the zinc is in a state other than the simple substitutional one [74]. The difference between the hole concentration and zinc atomic concentration can be as high as two orders of magnitude [75]. It has been proposed [76] that the zinc diffuses interstitially, in the same manner as zinc in GaAs. Once incorporated on to the lattice site it forms a neutral complex with two phosphorus vacancies. Positron lifetime measurements have shown that in pre-doped zinc InP, divacancies exist in the concentration predicted by this model [77].

The first report of the disordering of a GaInAsP–InP system lattice matched to InP was by Razeghi *et al.* [78] who zinc-diffused an $In_{0.75}Ga_{0.25}P_{0.5}As_{0.5}$–InP quantum well at a variety of temperatures and times. The interdiffusion process was monitored by observing the shift in the photoluminescence peaks. They found that in the InGaPAs–InP system, like the InGaPAs–GaAs system, the diffusion of zinc enhances the diffusion of the group III atoms. They also observed evidence for the intermixing of the group V elements at 700 °C. Since enhancement of the interdiffusion of the group III atoms moves the absorption band edge to lower energies, zinc IID would not be appropriate to the manufacture of transverse junction lasers [78] or waveguides [79].

To examine the enhancement of the diffusion of the group III and V elements Park *et al.* [80] annealed an $In_{0.72}Ga_{0.28}P_{0.39}As_{0.61}$–InP heterostructure. Their results confirm previous results. However, in their discussion they attempted to relate the diffusion mechanism for zinc in InP to the intermixing of the layers. (This is the only group which has taken this important step.) The first diffusion mechanism they discussed was that of Yamada *et al.* [81]. They noted that, if the defect responsible for the diffusion of zinc in InP and related compounds is Zn–V_i pairs, then one would expect a significant enhancement in the group V diffusion and this is not seen. They then considered the model proposed by Tuck and Hooper [76]. In this model the interstitial zinc when incorporated on to the lattice site requires two phosphorus vacancies. They assumed that these phosphorus vacancies must arise from the surface and would therefore have to diffuse, causing an enhancement of the group V diffusion. It should be stated, however, that the original model would still be valid if the vacancies were created by Frenkel pair production, and the diffusion of the group V interstitials is small in relation to the group III interstitial diffusion.

More recent work on InGaAs–InP multi-quantum well structures has shown that not only does intermixing occur but under the correct conditions the InP–InGaAs layers can be converted to Zn_3P_2–Zn_3As_2 layers by the diffusion of zinc [82–84]. Schwarz and co-workers [82, 83] were the first group to observe this effect in InGaAs–InP multi-quantum well systems. A SIMS profile of an $In_{0.53}Ga_{0.47}As$–InP multi-quantum well which was zinc-diffused for 1 h at 600 °C showed a large surface concentration of zinc and phosphorus (the zinc source was Zn_3As_2). Examination of the crater left by the SIMS analysis showed that there were islands which had a low sputtering yield. Schwarz *et al.* [82] verified that these islands were indeed Zn_3P_2. Although not mentioned by Schwarz *et al.*, Tuck and Hooper [85] have previously observed surface features on zinc-diffused InP samples (700 °C). These surface features depended critically on the external conditions. No features were observed for those samples which were diffused either with low amounts of zinc or with large amounts of phosphorus. Two types of surface feature were observed. For diffusion times in the region of 4 to 5 h the surface deposits took the form of hemispheres, ranging in size from a few micrometres to 0.25 mm. These hemispheres were found to be indium-rich. However, on samples diffused for 20 min different features were observed. These took a rectangular form and were aligned on the crystal surface. Chemical analysis of these features showed that they were zinc- and phosphorus-rich. Tuck and Hooper [85] explained their results with the aid of phase diagrams and as a consequence assigned the rectangular features to crystalline Zn_3P_2 and the hemispheres to the condensation of an indium-rich liquid.

The conversion of the InGaAs–InP layers to Zn_3P_2–Zn_3As_2 layers has been studied in more detail by Hwang *et al.* [83]. One of their SIMS profiles is reproduced in Fig. 12. In region 1, most distant from

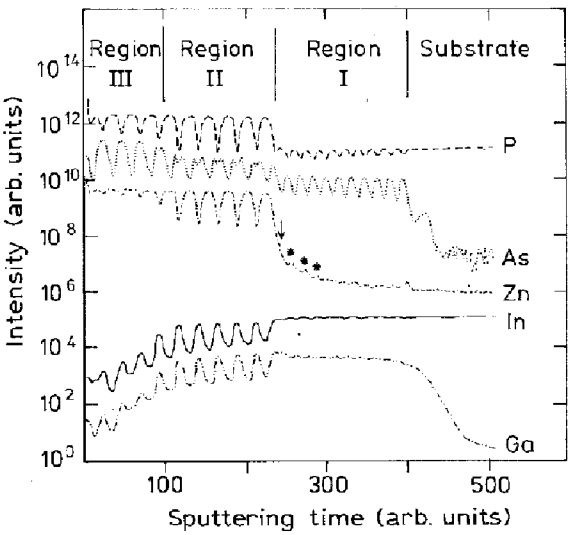

Figure 12 SIMS profile through a zinc-diffused InGaAs–InP superlattice performed at 600 °C for 20 min. The zinc-diffused area shows three regions. In region I, the group III elements have interdiffused but the group V elements are unaffected, whilst in region II the group III elements Ga and In have been replaced by zinc forming Zn_3P_2. The InGaAs layers are unaffected. Finally in region III close to the surface the InGaAs has been converted to Zn_3As_2 (after Hwang *et al.* [83]). (Reproduced with the permission of the American Institute of Physics.)

the surface, the group III atoms are interdiffused. The group V elements are relatively unaffected. In the middle region (region II) the InGaP has been converted to Zn_3P_2. The InGaAs layers remain intact. However, close to the surface, in region III, the InGaAs layers are converted to Zn_2As_3. They also noted that, as they increased the zinc pressure in the diffusion ampoule, more conversion of the layers was observed. This dependence on zinc overpressure confirms the observations of Tuck and Hooper [85].

Van Gurp *et al.* [84] have studied the diffusion of zinc in $In_{0.58}Ga_{0.42}As_{0.9}P_{0.1}$–InP at various temperatures (all diffusions used Zn_3P_2 as the diffusion source). As the diffusion temperature increases the capping InP layer is gradually changed to Zn_3P_2. This can be seen in Fig. 13, which shows Auger profiles for several zinc diffusions performed at different temperatures. The conversion to Zn_3P_2 was explained in terms of free energy. The heat of formation of InP is greater than that of Zn_3P_2. As a consequence there would be a gain in free energy when InP changes to Zn_3P_2.

In addition to the conversion of the top InP cladding layer, the indium and gallium start to interdiffuse (Fig. 13b and c). Initially Auger signals caused by the indium and gallium oscillate in the layered structure, demonstrating that no intermixing has occurred. At higher temperatures the indium and gallium signals are constant, indicating that intermixing has occurred. However, at 550 °C, oscillations in the gallium and indium Auger signal occur again (Fig. 13d). Moreover the maximum of the gallium signal, which corresponds to the minimum of the In, occurs in the layers which were originally InP. This surprising result indicates that ordering has occurred. van Gurp *et al.* [84] proposed that the ordering of the layers was again caused by the gain in free energy when InP is converted to InGaP. An interesting observation, not commented on by van Gurp *et al.*, can be seen in Fig. 13e. There is a rise in the zinc Auger signal. This occurs in what was the first InP layer and could be the start of the conversion of this layer to Zn_3P_2. This observation and explanation would be in agreement with Hwang *et al.* [83].

Ambree *et al.* [86] have studied the effects of diffusion over a long period on zinc and cadmium across an InGaAs–InP heterojunction. In the case of zinc, they found that there was significant zinc gettering at the heterojunction which was accompanied by a decrease in the indium and gallium concentrations. This did not occur for their cadmium-diffused samples.

4. Beryllium

Be diffusion in GaAs is believed to proceed by the kick-out mechanism. Owing to the health risks associated with beryllium there is little work concerning its in-diffusion. Poltoratskii and Stuchebnikov [87] diffused beryllium from sources evaporated on to the sample's surface. They found that the diffusion of beryllium depended on the amount of arsenic added to their diffusion ampoule. The diffusion of beryllium seems to be slower than that of zinc. The diffusion of beryllium from grown-in sources has been studied by Ilegrems [88] and McLevige *et al.* [89] who found that the diffusion coefficients obtained were significantly smaller than those obtained in the in-diffusion experiments. In addition, like zinc, the diffusion of beryllium is a concentration-dependent process [90]. The similarities between the diffusion of zinc and beryllium suggests that a similar diffusion process is occurring [91–93]. Recently, there has been some interest [94, 95] in the diffusion of beryllium away from δ-doped regions. The results were analysed in terms of a single concentration-independent diffusion coefficient. The diffusion coefficient obtained was several orders of magnitude less than in the earlier published work [88]. However, the concentration of the Be was significantly higher in the previous work.

Kawabe *et al.* [96] have found that superlattices doped to $2 \times 10^{19}\,cm^{-3}$ show little signs of disordering. Moreover they found that it prevented the disordering of the superlattice by the silicon. (It is now generally accepted that this is due to the lowering of the Fermi level.) However, Devine *et al.* [97] have shown that if beryllium-doped GaAs is grown so that the beryllium interstitials are not in equilibrium with the beryllium substitutional atoms, then diffusion during growth can occur which causes enhancement of the interdiffusion of the group III elements in a similar way to that of zinc.

5. Manganese and magnesium

Under certain conditions, the diffusion of manganese has many similarities to zinc diffusion. This led Kendal [98] to postulate that manganese and zinc have the same diffusion mechanism. One would therefore expect the diffusion of manganese to cause an enhancement of the interdiffusion of the gallium and

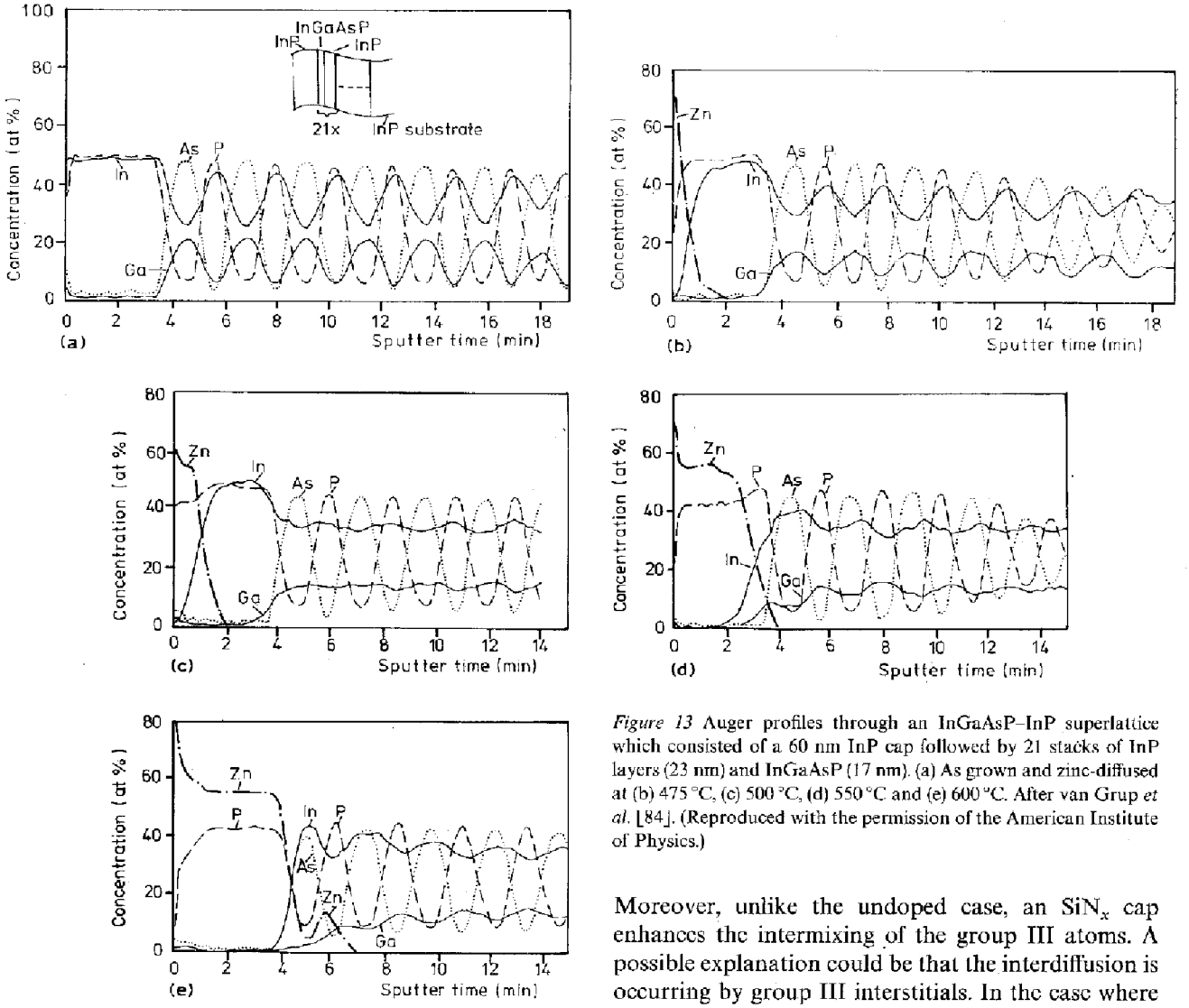

Figure 13 Auger profiles through an InGaAsP–InP superlattice which consisted of a 60 nm InP cap followed by 21 stacks of InP layers (23 nm) and InGaAsP (17 nm). (a) As grown and zinc-diffused at (b) 475 °C, (c) 500 °C, (d) 550 °C and (e) 600 °C. After van Grup *et al.* [84]. (Reproduced with the permission of the American Institute of Physics.)

aluminium in GaAs–AlAs superlattices. This has indeed been observed [99–102]. However, it should be noted that in these earlier experiments [101] there was a significant amount of surface degradation. In this work, only a solid Mn source was used along with a piece of elemental arsenic. The poor surface morphology following a manganese diffusion was also seen by Wu *et al.* [102] who used a variety of sources (elemental manganese, MnAs, Mn_3As and a thin film of manganese deposited on GaAs). However, only the MnAs source produced a smooth crystal surface.

There are few data for magnesium in GaAs. Small *et al.* [103] diffused Mg, from a liquid source, into GaAs at 830 °C. The magnesium profiles obtained by SIMS suggest that the magnesium diffusion coefficient is concentration-dependent. More recently, the effects of magnesium on the interdiffusion of GaAs–AlAs layers have been investigated [104, 105]. When a magnesium-doped (8×10^{18} cm^{-3}) $Al_{0.4}Ga_{0.6}As$–GaAs superlattice was annealed, with additional arsenic added to the ampoule, there were no signs of interdiffusion of the layers. This is in contrast to when the same structure was annealed without any As. In this case, the structure was completely disordered. This result is also seen when magnesium diffuses from a δ-doped region in a multi-quantum well [104].

Moreover, unlike the undoped case, an SiN_x cap enhances the intermixing of the group III atoms. A possible explanation could be that the interdiffusion is occurring by group III interstitials. In the case where there is a high arsenic overpressure, the concentration of group III interstitials will be low and so the intermixing should be small, whereas when the sample surface is gallium-rich (no arsenic provided), the opposite is true.

6. Silicon

Understanding the diffusion mechanisms of group IV dopants is severely complicated by their amphoteric nature. There has been a significant amount of work directed at establishing on which site the silicon atom sits (see for example [71, 106, 107]. For GaAs [0 0 1] it is generally accepted that, at low silicon concentrations ($< 10^{18}$ cm^{-3}), the silicon sits on the gallium site (Si_{Ga}) forming a donor. However at high concentrations, which are of interest in diffusion studies, the picture is less clear. Local vibration mode (LVM) studies of heavily doped silicon GaAs wafers show several other defects occurring, namely a silicon atom on an arsenic site (Si_{As}), an Si_{Ga}–Si_{As} pair, and two other defects which have been labelled Si–X and Si–Y. On annealing, the carrier concentrations changes. Chen and Spitzer [106] investigated this effect and they showed that all the changes they observed were reversible. As a starting material they used wafers which had undergone a 1200 °C thermal anneal and were then quench-cooled after 1 h (they demonstrated

that the carrier density after this anneal was independent of the sample's previous thermal history). These samples were then subjected to different thermal anneals. In general, the concentration of Si_{Ga} is seen to decrease after the second anneal whilst the concentrations of the Si–X and Si–Y defects increase. The effect of the anneal on the other defects depended significantly on the annealing temperature. After a 500 °C anneal there was a decrease in the concentration of Si_{As} and an increase in Si_{Ga}–Si_{As} pairs, whereas at 700 °C the concentrations of Si_{As} and Si_{Ga}–Si_{As} pairs remained approximately constant. To explain their results, Chen and Spitzer suggested the formation of an additional defect which was an acceptor. They proposed that this defect may be a Si_{Ga}–V_{Ga} pair. More recently, Theis and Spitzer [108] have suggested that the Si–X defect is an Si_{As}–V_{Ga} pair. As for the Si–Y defect, this was proposed to be an Si_{As}–As_{Ga} pair. More recent work [107] has come to the same conclusion as to the origins of the Si–X defect. For the Si–Y defect, however, Ono and Newman [109] suggest that the Si–Y defect acts like an acceptor and is possibly an Si_{Ga}–V_{Ga} pair. To confuse the issue even further, the Si–Y defect is not always seen. For example in the molecular beam epitaxy (MBE) samples used by Maguire *et al.* [110] absorption in the LVM spectrum due to the Si–Y defect was not observed.

It is with this confusion over the exact nature and relationship between the silicon defects that one has to review the proposed diffusion mechanisms for silicon. The first proposal for the diffusion mechanism of silicon was presented by Greiner and Gibbons [111, 112]. In their experiments silicon had been diffused from thin sputtered silicon films deposited on the surface of the GaAs sample which was then rapidly thermally annealed, and the amount of silicon diffusion was assessed by SIMS measurements. They noted that when their samples were capped with SiN_x, no silicon diffusion occurred. However, significant amounts of diffusion occurred when the sample was capped with SiO_2. One of their profiles is shown in Fig. 14. From this profile it can be seen that the silicon concentration rapidly falls off with silicon concentration, which is characteristic of a diffusion constant that is dependent on concentration. To explain their results, they drew on the knowledge of the amphoteric nature of silicon and postulated that the silicon diffused as Si_{Ga}–Si_{As} pairs. As can be seen in Fig. 14, their model fits their data very well.

More recently, experiments by Deppe *et al.* [113] have shown that the diffusion rate of silicon critically depends on the original doping level. There was very little silicon diffusion in the sample which was highly p-type doped, whereas in the sample which was lightly doped there is significant penetration of the silicon. To explain their results, Deppe *et al.* proposed that silicon diffuses by Si_{Ga}^{+} V_{Ga}^{-} pairs. In the p-doped material the concentration of V_{Ga}^{-} would decrease, thereby decreasing the amount of silicon diffusion. Later, it was found that in n-type GaAs the amount of silicon diffusion depended also on the type of dopant [114]. The amount of silicon diffusion was independent of the group VI dopant used; however, when tin was used

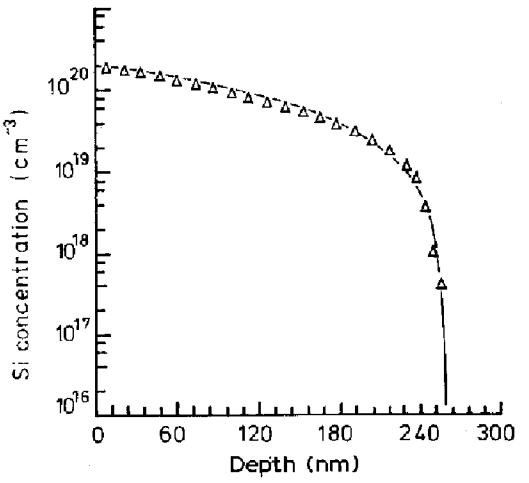

Figure 14 SIMS profile for a 1050 °C Si diffusion into GaAs with a calculated diffusion profile using the pair theory of Si diffusion (after Greiner and Gibbons [112]): (△) SIMS data, (——) model. (Reproduced with the permission of the American Institute of Physics.)

there was a significant increase in the silicon diffusion. These results were explained within the context of the Si_{Ga}^{+}–V_{Ga}^{-} model. They proposed [114] that the group VI elements formed complexes with the V_{Ga}, thereby reducing the V_{Ga} concentration and so slowing the silicon diffusion. The Si_{Ga}^{+}–V_{Ga}^{-} model also explains why when Greiner and Gibbons used an SiN_x cap no diffusion was observed. The solubility of gallium in SiO_2 is known to be very high and so one would therefore expect a large concentration of gallium vacancies at the SiO_2–GaAs interface which would increase the population of Si_{Ga}^{+}–V_{Ga}^{-} pairs. This would in turn increase the silicon diffusion. SiN_x, on the other hand, is relatively impervious to gallium atoms and so one would not expect a large concentration of V_{Ga} at the interface and so a small silicon diffusivity is expected.

Kahen [115] derived an expression for the effective silicon diffusion coefficient for the Si_{Ga}–V_{Ga} pair model and the model was fitted to previously obtained experimental data [111, 116]. These fits are shown in Fig. 15 and it can be seen that the two agree.

A third diffusion mechanism for silicon has been proposed [117]. In this model, the silicon had three ways of diffusing: (i) as Si_{Ga}^{+} via uncharged defects, (ii) as Si_{Ga}^{+} via a triply charged defect, probably V_{Ga}^{3-}, and (iii) as Si_{As}^{-} via a triply charged defect. Fits of this model to experimental results again showed very good agreement between the measured profiles and the theoretical ones. However, it still is unclear how the Si_{As}^{-} diffuses. The mathematical description of the model is valid for diffusion mechanisms based around either V_{As} or I_{As} [117] but theoretical calculations [118] show that these defects are positively charged and so do not fit the necessary requirements for the model [117].

The Si_{Ga}–Si_{As} pair model has in its favour the fact that the Si_{Ga}–Si_{As} defect pairs are observed in the LVM absorption loss spectra discussed above. It is not directly clear how the effect of p-doping on the silicon diffusion could be explained. However, under the p-doping condition one would expect the formation of Si_{As}^{-} to be very unlikely and therefore the

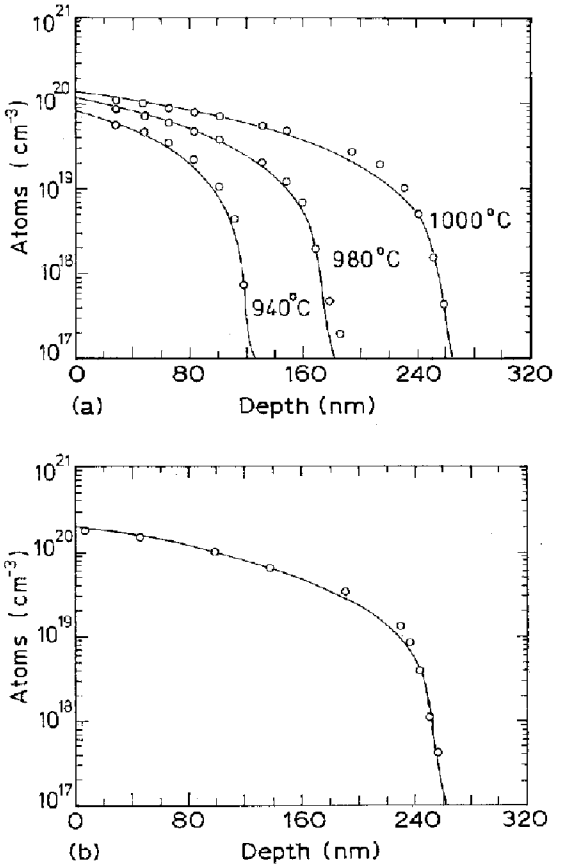

Figure 15 Comparison between experimental results and theoretical Si diffusion profiles obtained with the Si_{Ga}–V_{Ga} model (after Kahen [115]): (a) 10.0 s, (b) 3.0 s at 1050 °C. (Reproduced with the permission of the American Institute of Physics.)

concentration of Si_{Ga}–Si_{As} pairs would be expected to be small. In the initial work of Greiner and Gibbons [112] silicon and Ge were diffused together. The concentration profiles were remarkably similar and this was used as evidence for the formation of the pairs. A similar process could explain the dependence of the silicon diffusivity on the donor species, i.e. the silicon could be pairing with the tin atoms. It should be stressed that when the Si–Ge source was used the diffusion front was retarded relative to the pure silicon source case.

If the LVM assignments of Ono and Newman [109] are believed then the Si–Y defect which has been assigned to the Si_{Ga}^{+}–V_{Ga}^{-} defect is not observed in many silicon-doped samples. One would certainly expect to see defects of this kind in highly doped silicon samples if the diffusion of silicon occurred by Si_{Ga}^{+}–V_{Ga}^{-} pairs. Recently, Lee *et al.* [119] concluded that silicon most likely diffuses by V_{Ga}^{-}. Furthermore, positron annihilation experiments [120] suggest that the concentration of V_{Ga}^{-} increases with silicon doping. These experiments suggest that the assignment of Si–Y may be incorrect.

The model proposed by Yu *et al.* [117] appears to fit the experimental data better than the other two models. This may however be due to the increased number of fitting variables used. Moreover, it does not take into account the formation of silicon-related defects which are present in highly silicon doped GaAs.

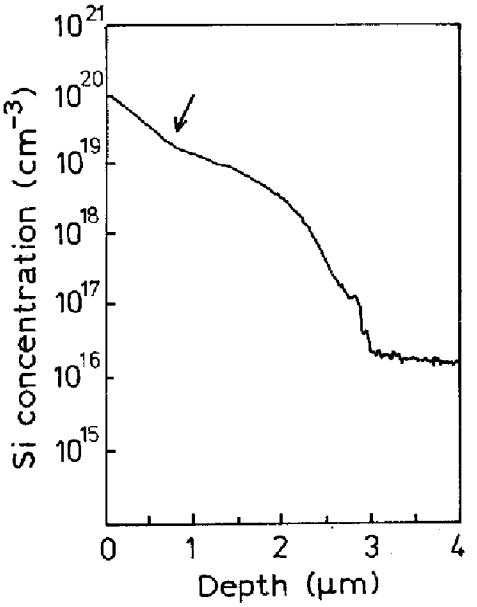

Figure 16 Diffusion profile of a 900 °C Si diffusion which shows the concave section (marked with an arrow) which is characteristic of the breakdown in the equilibrium concentrations of the crystal defects governing the diffusion (after Lee *et al.* [119]). (Reproduced with the permission of the American Institute of Physics.)

In all the models mass action has been applied, which essentially means that equilibrium is being implicitly assumed. However, the profiles presented by Lee *et al.* [119], an example of which is shown in Fig. 16, are similar to those obtained in sulphur-diffused GaAs, namely the profile contains a concave section which is marked with an arrow. It has been proposed that the origin of the sulphur double profiles was a breakdown in equilibrium within the crystal [3]. A similar effect may be occurring in silicon-diffused samples.

6.1. GaAs–AlAs

Si-induced disordering of GaAs–AlAs superlattices is a well-known phenomenon [121, 122]. The enhancement of the interdiffusion of the group III elements can be achieved either by in-diffusion of the silicon [122] or from a grown-in source [121]. The first systematic study of diffusion-induced disorder was performed by Mei *et al.* [10]. In this series of experiments regions of a 10 nm AlAs–40 nm GaAs superlattice were selectively doped and annealed. The SIMS profile of the as-grown specimen is shown in Fig. 17a and the silicon doping levels were 2×10^{17}, 5×10^{17}, 1×10^{18}, 2×10^{18}, 5×10^{18} cm^{-3} and finally 2×10^{18} cm^{-3} again. Fig. 17b and c show the SIMS profiles of the Mei *et al.* samples after a 700 °C and a 900 °C anneal. The annealed samples clearly show that there is an enhancement of the interdiffusion of the group III elements at high silicon concentrations. By measuring the peak to valley ratios of the SIMS profile, Mei *et al.* [10] were able to derive a figure for the aluminium interdiffusion coefficient for each doping level at each annealing temperature. To obtain an activation energy for the aluminium interdiffusion they assumed that the doping effect on the interdiffusion only affected the pre-exponential term, and

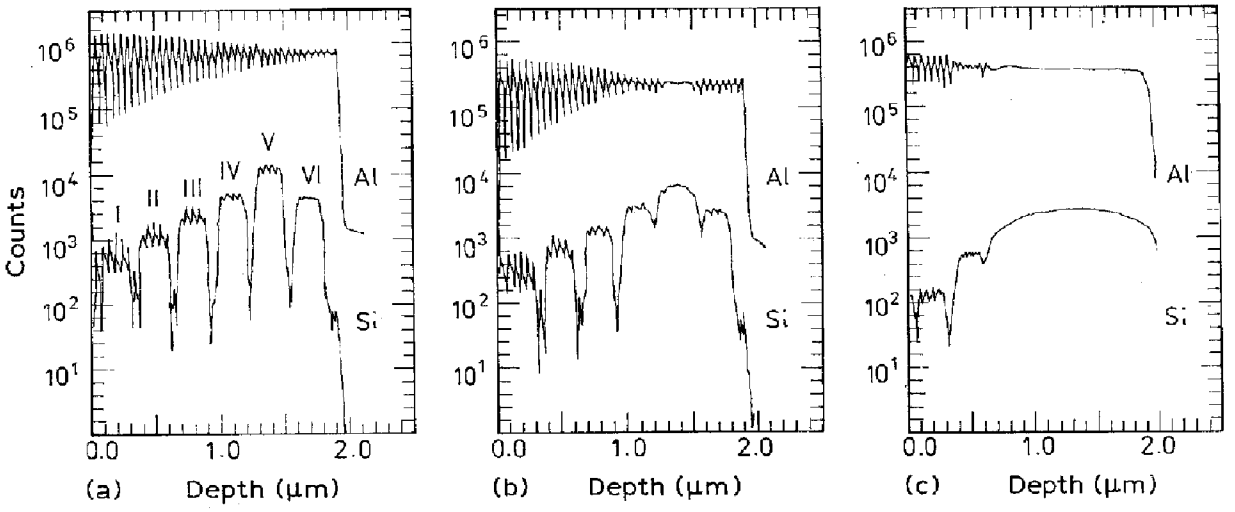

Figure 17 SIMS depth profiles of Al and Si for samples which have been selectively Si-doped to a level of 2×10^{17}, 5×10^{17}, 10^{18}, 2×10^{18}, 5×10^{18} and 2×10^{18} cm^{-3}; (a) shows the as-grown sample, whereas (b) and (c) show the profiles of samples after a 3 h 700 °C and a 3 h 900 °C anneal, respectively (after Mei *et al.* [10]).

they obtained a value of 3.8 eV for the activation energy. It should be noted, however, that at low silicon doping (2×10^{17} cm^{-3}) the fit was very poor. By using their model, Mei *et al.* were able to adjust their results so that they could compare the aluminium interdiffusion coefficient as a function of the silicon concentration; it is not clear, however, whether this refers to the actual silicon concentration or the concentration they intended to grow-in (Fig. 18). They showed that the interdiffusion varies as the third power of the silicon concentration.

Later the same group performed a similar experiment but at higher doping levels [123]. At 10^{20} cm^{-3} they observed that the intermixing of this region was less than that in the neighbouring region which was doped with 10^{19} cm^{-3}. Moreover, in a region which was doped to 10^{19} cm^{-3} dislocation loops were observed. It is well known [124] that at high silicon concentrations the electrical activity drops. This provides evidence for the Fermi-level effect (see below). However, Mei *et al.* [123] also noticed that the diffusion of the silicon had been suppressed. All the silicon models described above when coupled with the apparent lowering of the Fermi level could explain the reduction in the silicon diffusivity. However, at high silicon concentrations, the silicon may be in a different form which results in compensation and so there will be a lowering of the Fermi level. This new form of the silicon may be less mobile, which would explain the suppression of the silicon diffusion. The current feeling of the literature is that the first explanation is the correct one but the latter cannot be discounted.

There are at present two mechanisms which have been proposed to explain the interdiffusion of the AlAs–GaAs quantum wells. The first was put forward by Tan and Gösele in 1987 [9]. This model accounts for the intrinsic interdiffusion as well as the interdiffusion under n-type doping. They proposed that the interdiffusion in both cases has a common cause, namely a triply negatively charged gallium vacancy. The concentration of this vacancy would increase with n-type doping, thereby causing an increase in the

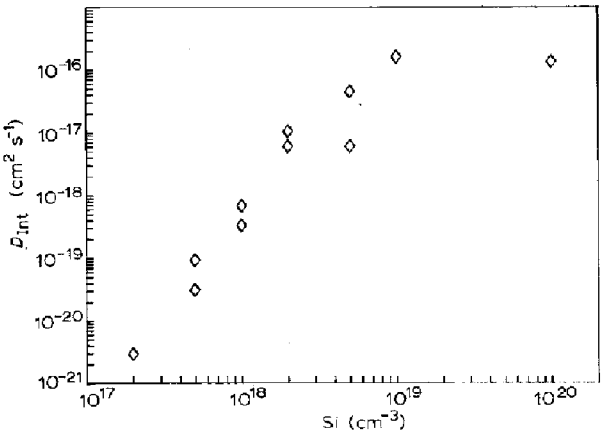

Figure 18 Al interdiffusion coefficient as a function of Si concentration (data from Mei *et al.* [10, 123]).

observed interdiffusion. The triple charged nature of the gallium vacancy explains why a log–log plot of the aluminium interdiffusion coefficient against silicon concentration has a gradient of 3. However, the results obtained for tellurium, where the corresponding log–log plot has a gradient of unity, suggest that this theory is not as universal as the proposers suggest [125, 126].

The other explanation, very similar to the first, put forward to explain the intermixing was a natural extension to the Si_{III}–V_{III} model of silicon diffusion [127]. As the Si_{III}–V_{III} defect diffuses through the crystal there will be an enhanced diffusion of the group III vacancy which in turn will increase the interdiffusion coefficient of the group III elements. The concentration of the Si_{III}–V_{III} pair depends not only on the concentration of the Si_{III} but also the concentration of the charged V_{III}, so the pair concentration will be dependent on the position of the Fermi level. The nearer the conduction band, the greater the concentration of charged V_{III} and hence Si_{III}–V_{III} pairs.

There is strong evidence to suggest that the Fermi-level effect plays an important role in the enhancement of the interdiffusion for silicon-doped superlattices.

The first signs of this came from Kawabe *et al.* [96] who annealed a multi-quantum well sample which was uniformly doped with silicon. The beryllium doping, however, varied. In the region where the beryllium doping exceeds the silicon concentration, which is presumably p-type, the intermixing was inhibited. In the other silicon-doped regions the expected intermixing was observed. More recently in implanted samples, the intermixing near the surface has been found to be inhibited. This was assumed to be due to Fermi-level pinning at the surface. Experimental verification of the pinning effect on the disordering has been observed [128]. The observed inhibition of the disordering near the surface correlated with the surface depletion layer. It should be noted, however, that the size of the effect was sometimes quite small. In addition, the exact surface conditions are unknown since the experiment was performed in flowing hydrogen with face-to-face contact with a piece of GaAs.

More recently still, silicon δ-doped samples have attracted interest both from the silicon doping [129, 130] and the disordering [131] points of view. There seems to be some confusion over the magnitude of the silicon diffusion coefficient. The initial results [132] indicated that the diffusion coefficient compared well with those obtained by Greiner and Gibbons [111, 112]. However, later results [130] indicated that the observed silicon diffusion coefficient was significantly smaller than that obtained by Greiner and Gibbons. The method used, *C–V* profiling, however only monitors the electrical concentration rather than the actual silicon concentration.

As far as the author is aware there are no data concerning the diffusion of silicon into InP or InAs. There are, however, a few data concerning the interdiffusion effects. Deppe *et al.* [127] diffused silicon through three different heterojunctions. For all the samples there was considerable group III intermixing with little group V intermixing. They interpret these results in terms of the Si_{III}–V_{III} model which they had proposed to explain silicon diffusion in GaAs–AlAs, since their model predicts that interdiffusion of the group V sublattice should not occur. The inherent assumption that they have made is that their silicon diffusion model is valid for the wide range of III–V compounds used in their study. Since there are no data for silicon diffusion in these compounds, their assumption that the silicon diffusion mechanism and the cause of intermixing are the same in all the III–V compounds studied is a good starting point. In a similar way one could just as well have applied the model of Tan and Gösele to explain the intermixing.

6.2. InAlAs–InGaAs

Si-induced disordering of InAlAs–InGaAs has been observed by Miyazawa *et al.* [133] who grew several samples of differing silicon concentration. The samples were annealed at 650 or 700 °C in close contact with a piece of GaAs for various times. The amount of intermixing was assessed by sputter Auger profiling and photoluminescence. The sample with a doping level of 7×10^{18} showed little signs of disorder after a 2 h anneal at 700 °C. This is in contrast to the sample doped at 1.3×10^{19} cm^{-3} which showed significant disordering. These results indicate that the silicon-induced disordering in InGaAs–InAlAs is, like GaAs–AlAs, highly dependent on the silicon concentration. From the work of Mei *et al.* [10] on silicon-induced disordering in GaAs–AlAs, one would expect GaAs–AlAs superlattices to show large amounts of disordering at the 7×10^{18} cm^{-3} doping level used by Miyazawa *et al.* [133]. This indicates that the silicon-induced disordering process in InGaAs–InAlAs occurs at higher silicon levels or is slower than the similar process in GaAs–AlAs. The mathematical representation of the Tan and Gösele Fermi-level theory [9] is given by

$$D(n) = D(n_i)\left(\frac{n}{n_i}\right)^3 \tag{4}$$

where $D(n)$ is the interdiffusion coefficient under a doping n and $D(n_i)$ is the interdiffusion coefficient under intrinsic conditions. Assuming that the Fermi-level theory applies to all III–V semiconductors [12], one can obtain an estimate of the silicon-induced interdiffusion coefficient. This is given by

$$\frac{D_I(n)}{D_G(n)} = \frac{D_I(n_i)\, n_G^3}{D_G(n_i)\, n_I^3} \tag{5}$$

The subscripts I and G refer to the InGaAs–InAlAs system and the GaAs–AlAs system, respectively. This equation cannot be used accurately since there is a large uncertainty in obtaining not only n_i at diffusion temperatures for both systems but the lack of information concerning the interdiffusion under intrinsic conditions of the InGaAs–InAlAs. However, an estimate of the size can be obtained. The differences in n_i will be primarily due to the differences in band gap. Using the band gap values of GaAs and InGaAs one obtains a ratio of 10^{-4} for the ratio of n_{iG} and n_{iI}. Approximate values for the interdiffusion coefficient under intrinsic conditions can be obtained from the work of Tan and Gösele [12] and by extrapolating the results of O'Brien *et al.* [38]. Performing this one obtains from Equation 5 that the interdiffusion coefficient under similar n-type conditions in InGaAs–InAlAs will be less than that of GaAs–GaAlAs, which is in agreement with the experimental results presented above. This indicates that the model proposed by Tan and Gösele could explain the silicon intermixing of InGaAs–InAlAs.

6.3. InGaAs–InP

Silicon diffusion into InGaAs–InP multi-quantum wells has been studied by Schwarz *et al.* [82] who diffused silicon from a surface source and studied the interdiffusion effects by SIMS. Their SIMS profile is presented in Fig. 19. The intermixing only occurs in a small range of silicon concentrations centred around 5×10^{18} cm^{-3}. If disordering itself was only limited to a range of silicon concentrations then one would still expect the near-surface region to be intermixed, because at some stage of the diffusion the concentration of the silicon in the near-surface region must have

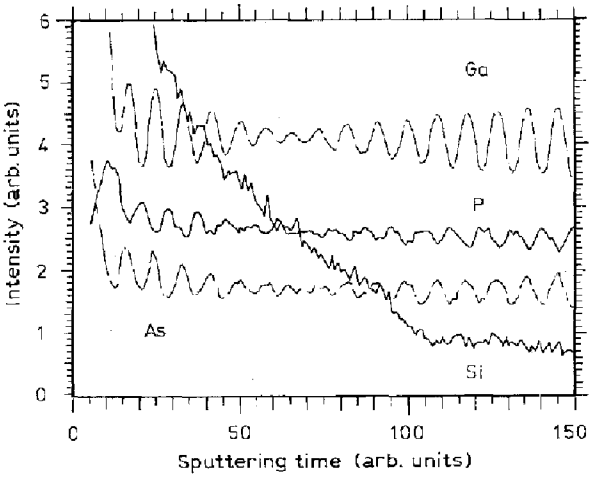

Figure 19 SIMS concentration profile of an InGaAs–InP superlattice which has been Si-diffused at 700 °C for 3 h (after Schwarz *et al.* [82]). (Reproduced with the permission of the American Institute of Physics.)

been in the appropriate range to cause disordering. The most likely cause of the inhibition of the intermixing near the surface is the pinning of the Fermi level at the surface. This effect has been observed in GaAs–GaAlAs. It is also interesting to note that the silicon diffusion causes intermixing on both the group III and the group V sublattices. This is in contrast to the work of Deppe *et al.* [127].

7. Tin

Tin diffuses slowly in GaAs. There have been two models put forward for the diffusion mechanism. Tuck and Badawi [134] diffused tin into undoped and n-type GaAs. At low temperatures, the diffusion coefficient of tin in n-type samples was significantly greater than in undoped samples. At higher temperatures the diffusion coefficients for the two samples were the same. This suggested that tin diffuses via negatively charged gallium vacancies. More recently Shaw [135] has proposed a different model. In his model, the tin diffuses via a complex ($V_{Ga}SnV_{Ga}$).

Disordering caused by tin is clearly shown in Fig. 20, which shows the disordering caused by the in-diffusion of the Sn [136]. In addition, the figure shows that increasing the arsenic overpressure inside the diffusion ampoule increases the amount of intermixing. It can also be seen that there is a correlation between the intermixing and the Sn. One could use the diffusion mechanism proposed by Shaw to explain the intermixing. As the $V_{Ga}SnV_{Ga}$ complex moves through the lattice one would expect an increase in the intermixing because of the increase in the V_{Ga} diffusion. (This is similar to the Si–V_{Ga} mechanism proposed for silicon-induced disordering.) However, it should be stated that the results obtained are consistent with the mechanism proposed by Tan and Gösele [9]. Rao *et al.* [137] have shown that boron implantation into a tin-doped superlattice inhibits the disordering. Since boron is isoelectronic with gallium no definite explanation could be given. However, they did suggest that under certain circumstances B could act as an acceptor. If this is correct then the Fermi-level effect may be the cause of the observed effect.

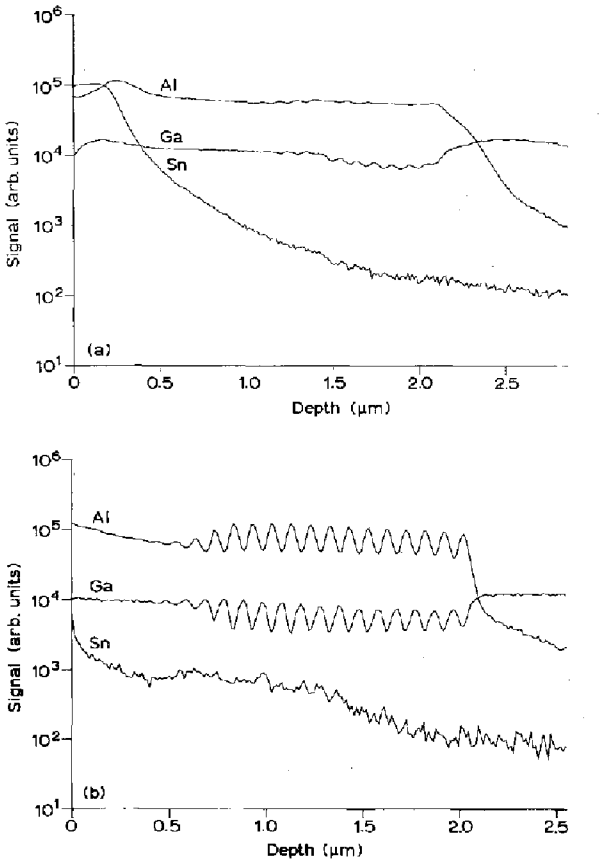

Figure 20 Effect of As overpressure on the Sn-induced disordering of GaAs–AlAs; (a) shows the effect of high As overpressure whilst (b) shows that of low As overpressure.

8. Germanium and carbon

There are very few data concerning the diffusion of Ge into GaAs. It has been noticed, however, that the Ge diffusion profile after a 10 h 800 °C diffusion was very similar to that of Si [138]. It is therefore not unreasonable to assume that Ge and silicon have similar diffusion mechanisms. Information concerning Ge-induced disordering of the AlGaAs GaAs layers is limited. However, devices have been fabricated using the effect [138].

Carbon diffusion in GaAs has been investigated by Cunningham *et al.* [139] who used a thin layer of highly doped GaAs as a diffusion source. The effects of background doping and masking materials were investigated. Carbon sits on the arsenic sublattice and acts as an acceptor. It was found to have a very small diffusion coefficient when compared with the diffusivity of Si, another group IV element, or zinc which is an acceptor. Carbon diffusivity was the greatest in p-type GaAs, whereas in n^+-GaAs there was no observable diffusion.

The same group [140, 141] has investigated the intermixing of carbon-doped AlGaAs–GaAs superlattices. These experiments are extremely interesting since the carbon is sitting on the group V lattice site. If the intermixing effect was purely due to the effect of the dopant on the Fermi level as proposed by Tan and Gösele, [ ] then the intermixing results obtained should be the same as those obtained for the magnesium-doped superlattices described above. However,

they found that, unlike magnesium-doped superlattices, the intermixing of the layers was increased when the samples were annealed in an arsenic-rich environment. In addition, they observed that the interdiffusion coefficient obtained for the sample which was annealed with an SiO_2 mask was only slightly less than that obtained from the sample with no cap. Furthermore, they noticed that the disordering under an SiN_x mask was significantly less. The interdiffusion coefficient obtained from these samples was approximately an order of magnitude less. To explain their results, they suggested that interstitial arsenic (I_{As}) and arsenic anti-site (As_{III}) defects could play a role in the interdiffusion process. They tentatively proposed that under arsenic-rich conditions the reaction below would move to the right:

$$I_{As} \rightleftharpoons AS_{III} + I_{III}.$$

This would increase the concentration of group III interstitials and hence the interdiffusion.

9. Selenium and tellurium

There is little reliable work on the diffusion of selenium and tellurium into GaAs and the diffusion mechanisms are still unknown [3]. The effect on the stability of GaAs–AlGaAs superlattices of selenium doping has been investigated by Deppe *et al.* [113]. The results they obtained qualitatively agree with the results of silicon, that is the disordering is enhanced when the sample is annealed in an arsenic-rich environment. In addition to the TEM pictures of the superlattice, which showed disordering, they presented carrier concentration profiles. For the sample which was annealed in an arsenic-rich atmosphere, the carrier concentration was reduced from that of the As-grown sample. This reduction of the carrier concentration was assigned to the in-diffusion of gallium vacancies which are generally assumed to be acceptors. Furthermore they noted that, in some of their TEM results, the layer interdiffusion was more complete near the bottom of the superlattice than at the crystal surface. They noted that these layers had a longer thermal anneal during growth which could have caused the increase in the intermixing.

The induced disordering of GaAs–AlAs superlattice has been investigated by Mei *et al.* [125, 126]. The experiment they performed was similar to the one they used to study silicon-induced disordering [10]. Different parts of a GaAs–AlAs superlattice were doped with different amounts of tellurium and the intermixing of the layers caused by post-growth anneals was monitored by SIMS. A value for the interdiffusion coefficient was obtained from the peak/valley ratios. They found that when the Ga–Al interdiffusion coefficient and the tellurium concentration were plotted on a log–log graph there was a linear dependence, the slope of the line being unity. For silicon, the slope was found to be 3. These results imply that the Ga–Al interdiffusion coefficient in tellurium-doped superlattices varies linearly with the tellurium concentration. This is in contrast to silicon-doped superlattices where the interdiffusion of the layers varies as the cube of the silicon concentration. If the Fermi-level model as proposed by Tan and Gösele were operative [12] one would expect the amount of disordering to be independent of the dopant, which is not the case. The interaction between the dopant atom and a group III vacancy will depend on the dopant species. The tellurium sits on the group V site and is thought to have a strong interaction with the group III vacancy [142], whereas for silicon, most of the silicon sits on the group III lattice site and interacts only weakly with the group III vacancies, thereby allowing the group III vacancy to move more freely and so cause more disordering. Further work is required to clarify this situation.

10. Sulphur

Sulphur diffusion in GaAs has been studied by a variety of workers (see Tuck [3] for references). Young and Pearson [143] obtained the sulphur diffusion coefficient in GaAs as a function of arsenic pressure. To explain their results they concluded that the sulphur diffused by a complex which consisted of a sulphur atom and two gallium vacancies ($V_{Ga}S_{As}V_{Ga}$). However, they could not explain the variation of sulphur solubility with sulphur pressure. This was later confirmed by Tuck and Powell [144]. Two very important details come from these studies: (i) there is not a one-to-one correspondence between the sulphur concentration and the electron density (this is often assumed when the diffusion is studied solely by electrical methods [145]), and (ii) many of the diffusion profiles cannot be described by a simple complementary error function.

Sulphur-induced disordering was investigated by Rao *et al.* [146] who diffused sulphur into a $Ga_{1-x}Al_xAs$–GaAs superlattice in a partially closed graphite boat. From the shift in the photoluminescence line they observed the intermixing of the layers. Later Shieh *et al.* [147] confirmed this result and in addition studied the size of the transition region from disordered to ordered region. Even though the electrical profile of the diffused sulphur is very gradual, the transition region is very sharp, less than 100 nm. This compares with values of 200 and 50 nm for zinc and silicon, respectively [147].

Since sulphur, like other group VI elements, sits on the group V site, it could affect the diffusion of the group V elements. Major *et al.* [148] investigated this by using a superlattice which was modulation-doped with carbon. Any increase in the group V diffusion should be observable through the carbon signal. They found that the sulphur diffusion did not affect the carbon distribution. SIMS measurements indicated that sulphur had diffused into the sample but the doping level was not given. Moreover, they investigated the diffusion of sulphur into a selenium-doped superlattice. This was to decouple the diffusion from the Fermi-level effect. They observed that there was less disordering associated with the sulphur diffusion when the sample was unmasked then when an SiO_2 mask was used. They therefore concluded that the disordering caused by sulphur diffusion was due to the

TABLE II A summary of silicon implantation-induced disordering of GaAs–GaAlAs superlattices

Energy (keV)	Dose (cm^{-2})	Temperature (K)	Comments	Ref.
375	10^{14}		First report of Si ions causing disordering	[150]
80	10^{16}		Si level diffuses quickly above 3×10^{18} and the disordering only occurs with this diffusion	[151]
80	3×10^{14}–10^{16}	R.T.	More damage in the GaAs than the AlGaAs	[152]
180	3×10^{13}–3×10^{15}	R.T.	Heavy damage near the surface inhibits intermixing	[153]
80/160	10^{13}–10^{15}		Defects can suppress the intermixing	[154]
180	3×10^{15}	Various	The near-surface inhibition is not seen in samples implanted at high temperatures	[155]
800 + 400	$2 \times 10^{14} + 5 \times 10^{13}$		Interstitial loops are observed in the implanted areas	[156]
80	3×10^{14}–10^{16}	R.T.	GaAs preferentially damaged	[157]
100	3×10^{14}	77/293/483	Si-induced disordering was found to be anisotropic	[158]
160	2×10^{14}–2×10^{15}		Focused ion beam: effects of scan speed	[159]
160, 160 + 40	3×10^{15}–3×10^{15}		Optimum dose 3×10^{14}	[160]
50	2×10^{14}–10^{15}	R.T.	Totally disordered at 10^{15} cm^{-2}	[161]
220	3×10^{15}		Mathematical model presented	[162]
220	$\geqslant 10^{15}$	R.T.		[163]
1000	3×10^{14}–10^{16}	R.T.	Much higher doses are needed for disordering	[164]
220	3×10^{14}–3×10^{15}	R.T.	Correlation of defects and intermixing	[165]

diffusion of group III vacancies. The sulphur would diffuse causing an increase in the n-doping of the layer, which brings about an increase in the V_{III} solubility which in turn increases the vacancy diffusion from the surface and so an increase in the interdiffusion is observed. In their discussion section they assume that silicon and zinc at high doping levels produce compensated material. Yet it is well known that for GaAs, the hole concentration and zinc concentration agree within experimental error. In addition, it is implied that sulphur does not produce compensated material, which is in disagreement with the work of Young and Pearson [143].

A more detailed study of the effect of sulphur diffusion on a GaAs AlAs superlattice has been performed by Baba-Ali *et al.* [149]. They diffused sulphur into a GaAs–AlAs superlattice for a variety of conditions. They varied both the sulphur overpressure as well as the arsenic overpressure and noted the effect on the superlattice layers. On several samples, which were diffused with moderate amounts of sulphur and arsenic in the ampoule, they noted that there was a brown surface layer. When this layer was analysed by photoelectron spectroscopy it was shown to contain predominantely aluminium and oxygen. However, there were significant amounts of sulphur contained in the layer. It is known that Al_2S_3 reacts with water vapour to form Al_2O_3 and H_2S. On breaking the ampoules a pungent smell was detected and so it was concluded that when the ampoule was broken the layer was originally Al_2S_3 which reacted with water vapour in the atmosphere to form Al_2O_3. Moreover, the amount of intermixing was found to be significantly greater for samples with this coating. TEM photographs of these samples (Fig. 21) showed that, near the surface of the crystal, there was a band of tangled dislocation lines. It was proposed that these dislocation lines were associated with the relief of stress caused by solidification of the surface layer on quenching. The additional disordering was caused by the increase in defect population by these dislocation lines.

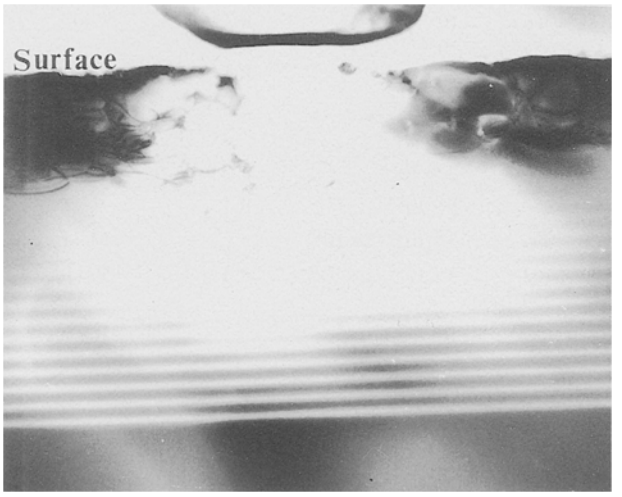

Figure 21 Cross-section TEM micrograph showing the tangled dislocation lines observed in S-diffused GaAs–AlAs superlattices [149]. Magnification × 20000.

11. Implantation

Implantation of dopants has several advantages over straightforward diffusion. The first is the likelihood of industry using this technique to incorporate the dopant in a device structure and secondly, it is possible to implant species which would be difficult to diffuse. There is however a disadvantage of using implant dopants. During the implantation process a significant amount of damage occurs to the crystal which disturbs the defect concentrations, and so it is difficult to obtain data pertinent to the intermixing caused by the dopant only.

As with the diffusion experiments the most studied system is the GaAs–AlAs system. Moreover silicon, which has a very low vapour pressure and is difficult to diffuse, has been the most popular dopant. In Table II the experiments so far performed on silicon-implanted GaAs have been summarized [150–178]. The disordering of a GaAs–AlGaAs superlattice was first observed by Coleman *et al.* [150]. After the implant, but before any thermal anneal, the layered structure of

TABLE III A summary of ion implantation-induced disordering of GaAs–GaAlAs

Ion	Energy (keV)	Dose (cm^{-2})	Temperature (K)	Comments	Ref.
Al Kr S	390 390 390	10^{14}–10^{15}		Both Kr, an inert atom and Al, a constituent atom, cause disordering	[165]
Be B F Si Ar As	60 65 125 200 200 200	8×10^{13} 8×10^{13} 8×10^{13} 8×10^{13} 6×10^{13} 3×10^{13}		A comparison of several dopants. Disordering efficiency Si > F > As > B > Ar > Be; Be does not cause disordering	[166]
Be Mg Si Se	80 40–140 60–140 100–175	5×10^{18} 2×10^{20} 2×10^{20} 3×10^{20}	R.T. R.T. R.T. R.T.	All showed signs of disordering except Be. Se the most efficient.	[167]
Ga	210	5×10^{12}–5×10^{13}	R.T.		[168]
Si S	100 100	2×10^{14} 2×10^{14}	77/R.T./210 77/R.T.	S was observed to cause only slight intermixing, if any.	[169]
Al	75/300	2×10^{13}–1×10^{15}	R.T.	Al causes disordering which is approximately 3 × greater than thermal annealing	[170]
Ga As Ge Si	344 366 355 150	10^{15} 10^{15} 10^{15} 10^{15}	R.T. R.T. R.T. R.T.	Comparative studies using SIMS	[171]
P	100	10^{15}	298/523	10 meV photoluminescence line shift achievable over annealed unimplanted	[172]
Ne	380	2×10^{16}	973	1 μm totally disordered	[173]
Ga	210	5×10^{13}	R.T.		[174]
As	35	5×10^{13}–5×10^{15}		Maximum shift at 2×10^{14}	[175]
Al Si	192 220/1000	3×10^{14}–1×10^{16}	R.T.	Voids are observed which prevent intermixing near the surface	[176]
B F		10^{14}–3×10^{15}		100 meV photoluminescence shift, low-loss waveguides	[177]
Ga	890–960	10^{13}–10^{15}	R.T.		[178]
Ar	150/250	4×10^{13}–7×10^{14}	77	Principally concerned with material-dependent amorphization	[180]
Ar				Ar sputtering and effects of different mask	[181]
Se	400	3×10^{12}–7×10^{13}	250		[182]
Ar	390	2×10^{13}–5×10^{14}	R.T.		[183]
Ga Zn Ar Mg Ne He	Various	Various	R.T.		[184]
O	2–500	1×10^{16}	100		[185]

the superlattice remained. However, there was a significant amount of lattice damage caused by the implantation process. Following a thermal anneal, which was performed with a temperature lower than the growth temperature, disordering of the superlattice was observed. The disordering was confined to a region in the middle of the superlattice from which Coleman *et al.* [150] concluded that the process was concentration-dependent. A later study by Fukunaga *et al.* [155] confirmed that the process was concentration-dependent (the larger the dose, the larger the amount of disordering). However, if the dose becomes too high there is considerable lattice damage caused by the incoming ions. This damage limits the disordering process. Again they observed that there was no intermixing in the sub-surface region. More recently, Chen *et al.* [176] using transmission electron microscopy have observed voids in the sub-surface layer which could explain the inhibition of the disordering in the sub-surface region. It is known from the work of silicon-induced disordering of GaAs GaAlAs superlattices that surface states pin the Fermi energy so that its approximate position is midway between the conduction and valence bands. Since the disordering of the superlattice requires the Fermi energy to be close to the conduction band, the effect of the surface states is to reduce the intermixing close to the surface. The effect has been observed in Si-doped GaAs–AlGaAs superlattices [128]. If the effect of the voids is also to pin the Fermi level midway between the conduction band and valence band one would expect an inhibition of the disordering. This is

TABLE IV A summary of ion implantation-induced disordering of systems other than GaAs–GaAlAs

System	Ion	Energy (keV)	Dose (cm^{-2})	Temperature (K)	Ref.
$In_{0.2}Ga_{0.8}As$–GaAs	N	75	10^{14}–2×10^{15}	R.T.	[188]
	Si	150			
	Zn	250			
$In_{0.14}Ga_{0.86}As$–GaAs	Si	150/350	5×10^{12}–10^{14}	R.T.	[189]
$GaAs_xP_{1-x}$–GaP	Be	75	10^{15}		[190]
$In_{0.53}Ga_{0.47}As$–$In_{0.52}Al_{0.48}As$	Si	200	5×10^{12}–5×10^{14}		[66]
$In_{0.53}Ga_{0.47}As$–$In_{0.52}Al_{0.48}As$	O	125	5×10^{13}–5×10^{14}	R.T.	[191]
	F	70			
$In_{0.53}Ga_{0.47}As$–$In_{0.52}Al_{0.48}As$	O	70/125	2×10^{14}–5×10^{14}	R.T.	[192]
	F	70			
	S	125			
InGaAs–InP	H				[193]
InGaAs–InP	P	100	10^{14}–10^{15}	R.T./473	[194]
InGaAs–InP	Si	200	3×10^{4}–5×10^{14}		[195]
InGaAs–InP	Ga	100	3×10^{3}–5×10^{14}	R.T.	[196]
InGaAs–InP	Ar	190	10^{15}	673	[197]
InGaAs(P)–InP	Ge	150–300	2×10^{14}–4×10^{14}	R.T.	[198]
	S	300	5×10^{14}		

not unreasonable, since voids are volumes inside the crystal which contain no atoms and so the interface between the crystal and the void could be acting as a "surface".

Table III shows a summary of the experiments which have been reported which used elements other than silicon. There have been two driving forces into the study of elements other than silicon. The first is to determine the relative contributions to the intermixing process of the collision-induced damage and the dopant effect. The second comes from the desire to find an element which when implanted causes disordering but introduces no free carrier. An element having these types of characteristic would be very useful for the manufacture of optical waveguides. It is interesting that beryllium does not cause an enhancement of the interdiffusion, whereas zinc, which is believed to diffuse in a similar way to Be, does [186]. This discrepancy is probably due to the difference in the amount of damage caused to the crystal by the implantation process. The lack of disordering caused by implanted beryllium has been used in the manufacture of semiconductor lasers [187]. The degree of understanding is significantly less in systems other than GaAs–GaAlAs (see Table IV).

12. Discussion

The theory of Tan and Gösele for the interdiffusion of GaAs–GaAlAs superlattices predicts, in general terms, what occurs in practice. However, the values of interdiffusion coefficients derived from their equations may be more than an order of magnitude out. There are several reasons which could account for this difference. In most of the experiments to date photoluminescence has been used to obtain an estimate for the interdiffusion coefficient. This analysis invariably assumes that Fick's law holds and the diffusion coefficient is independent of time and concentration. Early work of Chang and Koma [4] and Fleming *et al.* [5] clearly shows that the diffusion coefficient depends on the mole fraction of gallium. Moreover, latter studies [16, 199] have shown that the interdiffusion process is depth-dependent. When high As overpressure is used during the thermal anneal the surface concentration of V_{Ga} is above that in the bulk of the crystal and there is net diffusion of vacancies from the surface. Since the intrinsic diffusion mechanism is believed to occur by a simple substitutional mechanism which only involves the group III sites, the interdiffusion coefficient will depend on the concentration of vacancies. The observation of depth-dependent intermixing and the resulting explanation given above will make the measured interdiffusion coefficient time-dependent. With this important effect missing from the experimental analysis one would expect discrepancies between the measured and predicted values for the interdiffusion coefficients. This leads on to the second explanation for the discrepancies. To obtain a mathematical expression for the interdiffusion coefficient Tan and Gösele fitted self-diffusion data, interdiffusion data and data derived from Si interdiffusion work. The justification is that if Ga diffusion was the limiting factor in the interdiffusion process then one would expect the interdiffusion data and the self-diffusion data to agree [11]. They conclude that the fact that they obtain agreement between the self-diffusion data of Golstein and some of the available interdiffusion data is support for their conclusion. They later remarked that the agreement they obtained between the self-diffusion and the extrapolated interdiffusion coefficient was probably coincidental [12]. To obtain *a priori* information from the work of Mei *et al.* [10] one would need both the intrinsic interdiffusion coefficient, and the intrinsic carrier concentration at all the annealing temperatures. On the other hand if one assumes that the diffusion coefficient has the functional dependence of

$$D(n) = D(n_i)\left(\frac{n}{n_i}\right)^m$$

then one can obtain an estimate for both m and the intrinsic interdiffusion coefficient as long as the intrinsic carrier concentration is known. However, Tan

and Gösele [11] did not state how they derived the data from Mei *et al.* [10]. The fit of the experimental results to their model may be sufficient for Tan and Gösele to draw general conclusions, but not accurate enough for the device engineer who wishes to model the interdiffusion process. The observation that the intermixing of GaAs–GaAlAs superlattices depends on the crystal stoichiometry has extended our understanding of the interdiffusion process. It can also account for some of the discrepancies between the simple Tan and Gösele model [11] and the observed interdiffusion values. It is important to realise that material systems other than the GaAs–GaAlAs system will also have a dependancy on the crystal stoichiometry.

The effect of strain is yet to be fully understood. The system which has been analysed the most is the InGaAs–GaAs system. From the limited results so far obtained [39–43] it appears that increasing the strain increases the intermixing. All the results have a similar activation energy apart from those of Gillian *et al.* (Fig. 7). The experiment of Gillian *et al.* [41] was conceived to minimize the error due to variation of the photoluminescence line due to variations across the substrate, and unfortunately they introduced another one. In their experiments the samples were repeatedly heated and analysed. The logic behind this was simple. The evolution of the shift with time could be monitored and compared with that of the theory, and if the two agreed then one should have a good estimate of the interdiffusion coefficient. Unfortunately they overlooked the errors associated with the warming up and cooling down of the sample. The activation energy of their results should be higher than that of the other workers. Returning to the general comparison of the current work on InGaAs–GaAs, one possible explanation of the observed increase of the interdiffusion coefficient with strain is that the samples with the highest strain have the largest dislocation density, which means they will have the largest point defect sources, resulting in a larger interdiffusion coefficient.

For the InGaAs–InAlAs system, there have been reports of In diffusing from the barriers into the wells even though the molar concentrations in the well and barrier are approximately the same. One possible explanation is the effect of residual strain. I should like to advance an additional explanation. There could be a difference in the chemical potential between the InGaAs and the InAlAs which would result in diffusion of the In even though there is little or no concentration gradient. This difference in chemical potential could arise from differences in the heat of formation. A similar explanation has been advanced to explain the effect of diffusing zinc into InGaAs–InP [84].

There has been much discussion of the two contenders for the way in which zinc moves on to the substitutional lattice site. Several groups [200, 201] have attempted to distinguish between the two methods and have concluded that the two are indistinguishable. In reality the two are probably occurring in parallel. If one has a significant number of V_{Ga} then the zinc in all probability moves on to the lattice site via the dissociative mechanism, and if there is a shortage of the V_{Ga} then the kick-out mechanism prevails. This is supported by Pavesi *et al.* [202] who diffused zinc into an n-doped substrate and observed in their photoluminescence spectra an emission they assigned to $Zn–V_{Ga}$. It should be stressed that the dissociative mechanism requires the generation of Frenkel pairs to explain the intermixing process. The interdiffusion of GaAs–AlAs is believed to occur via the group III interstitials generated by the kick-out processes or the Frenkel pair production associated with the dissociative mechanism. The charge state of these interstitials is still open to question. The most favoured, at the moment, is a charge state of $+2$.

Zn diffusion in InGaAs–InP is very interesting and clearly indicates that diffusion processes are not simple, nor are they equilibrium ones. Moreover, it also demonstrates the need for phase diagrams. In this system, the zinc not only diffuses and disorders the InGaAs–InP but reacts chemically with it to form Zn_3P_2–Zn_3As_2 [82–84]. Tuck and Hooper [85] had previously observed this effect in Zn-diffused InP and could explain their results with the aid of the Zn–In–P phase diagram.

The fundamental cause of the enhancement of the interdiffusion in the n-doped superlattices is believed to be the Fermi-level effect suggested by Tan and Gösele [11]. There is, however, considerable debate over the exact way in which the Fermi level affects the intermixing. At first Tan and Gösele postulated that the intermixing process was governed by charged group III vacancies. The concentration of these vacancies would be drastically increased when the Fermi level approached the conduction band. This theory would be universal to all n-type dopants. A blow to this simple theory came with measurement of the interdiffusion of a GaAs–AlAs superlattice as a function of tellurium doping. The interdiffusion of the superlattice varied linearly with tellurium doping, which is in contrast to the case of silicon-doped superlattices where the interdiffusion coefficient varied as the cube of the doping concentration. To account for this difference it has been postulated that not all the tellurium is electrically active [20]. There is still a significant amount of work to be done on the n-doped superlattice. At the moment there is an over-reliance on one series of excellent experiments performed by Mei *et al.* [10, 123]. It is to this series of experiments that all other experiments are compared. Yet it is good experimental technique only to place this level trust in results which have been independently confirmed by other groups, preferably using a slightly different technique. There is therefore an urgent need to repeat the systematic work of Mei *et al.* and to extend the systematic studies to other dopants. This will provide the best test for the theory of Tan and Gösele [11] which should be valid for all n-type dopants. In addition similar systematic experiments should be extended to other material compounds. In the InGaAs–InP system, there is an addition complication of different group III and group V elements. Moreover, in this system, very little is known about the diffusion of silicon or any n-type dopant in these compounds. The effect of doping GaAs–GaAsSb with

silicon is very interesting. The interdiffusion of the layers reduces. This effect could also be explained by the use of the Fermi-level effect if the group V vacancy is positively charged. An increase in the Fermi level would decrease the concentration of charge vacancies; this in turn would lead to a reduction in the interdiffusion rate.

A similar effect should also be observed in InGaAs–InP but this may be difficult to observe, since it will be impossible to isolate the interdiffusion on each of the sublattices since they are coupled through the action strain.

13. Conclusions

The interdiffusion of III–V semiconductors has been discussed in the context of current diffusion theories and provides an insight into the subject. There is still much work to be performed before the subject is fully understood. The technological advances in devices (see for example [203–208]) has advanced much quicker than the understanding of the underlying physical phenomenon. This is to be expected when one considers the economical pressure for a marketable device to pay for the research. I would ascertain that the time has come for a systematic detailed study into the effect rather than the present scattered approach currently being pursued by most if not all the workers in the field. The founding systematic work of Mei et al. needs to be repeated to confirm their results and the studies extended to cover other dopants and material systems.

References

1. I. HARRISON, H. P. HO, B. TUCK, M. HENINI and O. H. HUGHES, *Semicond. Sci. Tech.* **4** (1989) 841.
2. W. D. LAIDIG, N. HOLONYAK Jr, M. D. CAMRAS, K. HESS, J. J. COLEMAN, P. D. DAPKUS and J. BARDEEN, *Appl. Phys. Lett.* **38** (1981) 776.
3. B. TUCK, "Atomic diffusion in III-V Semiconductors" (Hilger (IOP) Bristol, 1988).
4. L. L. CHANG and A. KOMA, *Appl. Phys. Lett.* **29** (1976) 138.
5. R. M. FLEMING, D. B. McWHAN, A. C. GOSSARD, W. WIEGMANN and R. A. LOGAN, *J. Appl. Phys.* **51** (1980) 357.
6. H. D. PALFREY, M. BROWN and A. F. W. WILLOUGHBY, *J. Electrochem. Soc.* **121** (1981) 2224.
7. *Idem., J. Electron Mater.* **12** (1983) 863.
8. B. GOLDSTEIN, *Phys. Rev.* **121** (1961) 1305.
9. T. Y. TAN and U. GÖSELE, *J. Appl. Phys.* **61** (1987) 1841.
10. P. MEI, H. W. YOON, T. VENKATESAN, S. A. SCHWARZ and J. P. HARBISON, *Appl. Phys. Lett.* **50** (1987) 1823.
11. T. Y. TAN and U. GÖSELE, 1987, *ibid.* **52** (1987) 1240.
12. *Idem., Mater. Sci. Eng.* **B1** (1988) 47.
13. L. J. GUIDO, N. HOLONYAK Jr, K. C. HSIEH, R. W. KALISKI, W. E. PLANO, R. D. BURNHAM, R. L. THORNTON, J. E. EPLER and T. L. PAOLI, *J. Appl. Phys.* **61** (1987) 1372.
14. A. FURUYA, O. WADA, A. TAKAMORI and H. HASHIMOTO, *Jpn. J. Appl. Phys.* **26** (1987) L926.
15. L. J. GUIDO, N. HOLONYAK Jr. and K. C. HSIEH, in Proceedings of International Symposium on GaAs and Related Compounds, Atlanta, Georgia, 1988, Institute of Physics Conference, Series No. 96 (1989) p 353.
16. N. BABA-ALI, I. HARRISON, B. TUCK, H. P. HO, M. HENINI and O. H. HUGHES, *J. Mater. Sci: Mater. Electron.* **1** (1990) 133.
17. K. Y. HSIEH, Y. C. LO, J. H. LEE and R. M. KOLBAS, in Proceedings of International Symposium on GaAs and Related Compounds, Atlanta, Georgia, 1988, Institute of Physics Conference, Series No. 96 (1989) p. 393.
18. R. M. COHEN, *J. Elec. Mater.* **20** (1991) 425.
19. *Idem., J. Appl. Phys.* **67** (1990) 7268.
20. T. Y. TAN, U. GÖSELE and S. YU, *Crit. Rev. Sol. Stat. Mater. Sci.* **17** (1991) 47.
21. *Idem., J. Appl. Phys.* **70** (1991) 4823.
22. B. L. OLMSTED and S. N. HOUDE-WALTER, *Appl. Phys. Lett.* **60** (1992) 368.
23. Y. SUZUKI, H. IWAMURA and O. MIKAMI, *ibid.* **56** (1990) 19.
24. J. WERNER, E. KAPON, N. G. STOFFEL, E. COLAS, S. A. SCHWARZ, C. L. SCHWARTZ and N. ANDREADAKIS, *ibid.* **55** (1989) 540.
25. J. Y. CHI, X. WEN, E. S. KOTELES and B. ELMAN, *ibid.* **55** (1989) 855.
26. X. WEN, J. Y. CHI, E. S. KOTELES, B. ELMAN and P. MELMAN, *J. Electron. Mater.* **19** (1990) 539.
27. T. YAMAMOTO, M. KASU, S. NODA and A. SASAKI, *J. Appl. Phys.* **68** (1990) 5318.
28. H. RIBOT, F. LARUELLE and L. A. COLDREN, *Appl. Phys. Lett.* **55** (1989) 2526.
29. T. E. SCHLESINGER and T. KUECH, *ibid.* **49** (1986) 519.
30. J. C. LEE and T. E. SCHLESINGER, *J. Vac. Sci. Technol.* **B5** (1987) 1187.
31. J. D. RALSTON, S. O'BRIEN, G. W. WICKS and L. F. EASTMAN, *Appl. Phys. Lett.* **52** (1988) 1511.
32. K. S. SEO, P. K. BHATTACHARYA, G. P. KOTHIYAL and S. HONG, *ibid.* **49** (1986) 966.
33. R. J. BAIRD, T. J. POTTER, G. P. KOTHIYAL and P. K. BHATTACHARYA, *ibid.* **52** (1988) 2055.
34. A. C. BRYCE, J. H. MARSH, R. GWILLIAM and R. W. GLEW, *IEE Proc. J.* **138** (1991) 87.
35. R. E. MALLARD, N. J. LONG, G. R. BOOKER, E. G. SCOTT, M. HOCKLY and M. TAYLOR, *J. Appl. Phys.* **70** (1991) 182.
36. T. MIYAZAWA, Y. SUZUKI, Y. KAWAMURA, H. ASAI and O. MIKAMI, *Jpn. J. Appl. Phys.* **28** (1989) L730.
37. J. Y. CHI, E. S. KOTELES and R. P. HOLMSTROM, *Appl. Phys. Lett.* **53** (1988) 2185.
38. O. S. BRIEN, J. R. SHEALY, D. P. BOUR, L. ELBAUM and J. Y. CHI, *ibid.* **56** (1990) 1365.
39. M. C. JONCOUR, M. N. CHARASSE and J. BURGEAT, *J. Appl. Phys.* **58** (1985) 3371.
40. G. P. KOTHIYAL and P. BHATTACHARYA, *ibid.* **63** (1988) 2760.
41. W. P. GILLIN, Y. S. TANG, N. J. WHITEHEAD, K. P. HOMEWOOD, B. J. SEALY, M. T. EMENY and C. R. WHITEHOUSE, *Appl. Phys. Lett.* **56** (1990) 1116.
42. J. S. MAJOR Jr, L. J. GUIDO, N. HOLONYAK Jr, K. C. HSIEH, E. J. VESELY, D. W. NAM, D. C. HALL, J. E. BAKER, P. GAVRILOVIC and K. MEEHAN, *J. Electron. Mater.* **19** (1990) 59.
43. K. Y. HSIEH, Y. L. HWANG, J. H. LEE and R. M. KOLBAS, *ibid.* **19** (1990) 1417.
44. H. TEMKIN, S. N. G. CHU, M. B. PANISH and R. A. LOGAN, *Appl. Phys. Lett.* **50** (1987) 956.
45. R. W. GLEW, J. P. STAGG, P. D. GREENE, A. T. R. BRIGGS, S. BRADSHAW and J. H. MARSH, presented at 3rd International Conference on InP and Related Materials, Cardiff, 1991.
46. S. J. YU, H. ASAHI, S. EMURA, S. GONDA and K. NAKASHIMA, *J. Appl. Phys.* **70** (1991) 204.
47. T. FUJII, M. SUGAWARA, A. YAMAZAKI and K. NAKAJIMA, *J. Cryst. Growth* **105** (1990) 348.
48. K. NAKASHIMA, Y. KAWAGUCHI, Y. KAWAMURA, H. ASAHI and Y. IMAMURA, *Jpn. J. Appl. Phys.* **26** (1987) L1620.
49. W. P. GILLIN, B. J. SEALY and K. P. HOMEWOOD, *Opt. Quantum Electron.* (1991) S975.
50. A. F. W. WILLOUGHBY, *Mater. Res. Soc. Symp. Proc.* **14** (1983) 237.

51. R. L. LONGINI, *Solid State Electron.* **5** (1962) 127.
52. U. GÖSELE and F. MOREHEAD, *J. Appl. Phys.* **52** (1981) 4617.
53. H. R. WINTELER, *Helv. Phys. Acta* **44** (1971) 451.
54. J. F. BLACK and JUNGBLUTH, *J. Elec. Chem. Soc.* **114** (1967) 181.
55. R. K. BALL, P. W. HUTCHINSON and P. S. DOBSON, *Phil. Mag.* **A43** (1981) 1299.
56. S. K. AGENO, R. J. ROEDEL, N. MELLEN, and J. S. ESCHER, *Appl. Phys. Lett.* **47** (1985) 1193.
57. C. P. LEE, S. MARGALIT and A. YARIV, *Solid State Electron.* **21** (1978) 905.
58. V. QUINTANA, J. J CLEMENCON and A. K. CHIN, *J. Appl. Phys.* **63** (1988) 2454.
59. Y. MATSUMOTO, *Jpn. J. Appl. Phys.* **22** (1983) 829.
60. S. E. BLUM, M. B. SMALL and D. GUPTA, *Appl. Phys. Lett.* **42** (1983) 108.
61. J. A. van VECHTEN, *J. Appl. Phys.* **53** (1982) 7082.
62. G. C. JAIN, D. F. SARDANA and B. K. DAS, *Solid State Electron.* **19** (1976) 731.
63. I. HARRISON, H. P. HO, B. TUCK, M. HENINI and O. H. HUGHES, *Semicond. Sci. Tech.* **5** (1990) 561.
64. B. I. BOLTAKS, T. D. DZHAFAROV, Y. P. DEMAKOV and I. E. MARONCHUK, *Sov. Phys. Semicond.* **9** (1975) 545.
65. I. HARRISON, *Int. J. Num. Mod.* **3** (1990) 91.
66. R. J. BAIRD, T. J. POTTER, R. LAI, G. P. KOTHIYAL and P. K. BHATTACHARYA, *Appl. Phys. Lett.* **53** (1988) 2302.
67. Y. KAWAMURA, H. ASAHI, A. KOHZEN and K. WAKITA, *Elec. Lett.* **21** (1985) 218.
68. B. TUCK and P. R. JAY, *J. Phys. D: Appl. Phys.* **10** (1977) 1315.
69. L. L. CHANG and G. L. PEARSON, *J. Appl. Phys.* **35** (1964) 374.
70. B. TUCK and P. R. JAY, *J. Phys. D: Appl. Phys.* **10** (1977) 1315.
71. M. D. CAMRAS, N. HOLONYAK Jr, K. HESS, M. J. LUDOWISE, W. T. DIETZE and C. R. LEWIS, *Appl. Phys. Lett.* **42** (1983) 185.
72. H. H. PARK, K. H. LEE and D. A. STEVENSON, *ibid.* **53** (1988) 2299.
73. D. G. DEPPE, D. W. NAM, N. HOLONYAK Jr, K. C. HSIEH, J. E. BAKER, C. P. KUO, R. M. FLETCHER, T. D. OSENTOWSKI and M. G. CRAFORD, *Appl. Phys. Lett.* **52** (1988) 1413.
74. R. M. KUNDUKHOV, S. G. METREVELI and N. V. SIUKAEV, *Sov. Phys. Semicond.* **1** (1967) 765.
75. B. TUCK and M. D. ZAHARI, in "Gallium Arsenide and Related Compounds"; Institute of Physics Conference, Series No. 33a (1976), 177.
76. B. TUCK and A. HOOPER, *J. Phys. D: Appl. Phys.* **8** (1975) 1806.
77. G. DLUBEK, O. BRUMMER, F. PLAZAOLA, P. HAUTOJARVI and L. NAUKKARINEN, *Appl. Phys. Lett.* **46** (1985) 1136.
78. M. RAZEGHI, O. ACHER and F. LAUNAY, *Semicond. Sci. Technol.* **2** (1987) 793.
79. I. J. PAPE, P. LI KAM WA, J. P. R. DAVID, P. A. CLAXTON, P. N. ROBSON and D. SYKES, *Electron. Lett.* **24** (1988) 910.
80. H. H. PARK, B. K. KANG, E. S. NAM, Y. T. LEE, J. H. KIM and D. O. KWON, *Appl. Phys. Lett.* **55** (1989) 1768.
81. M. YAMADA, P. K. TIEN, R. J. MARTIN, R. F. NAHORY and A. A. BALLMAN, *ibid.* **43** (1983) 594.
82. S. A. SCHWARZ, P. MEI, T. VENKATESAN, R. BHAT, D. M. HWANG, C. L. SCHWARTZ, M. KOZA, L. NAZAR and B. J. SKROMME, *ibid.* **53** (1988) 1051.
83. D. M. HWANG, S. A. SCHWARZ, P. MEI, R. BHAT, L. VENKATESAN, L. NAZAR and C. L. SCHWARTZ, *ibid.* **54** (1989) 1160.
84. G. J. van GURP, W. M. van de WIJGERT, G. M. FONTIJN and P. J. A. THIJS, *J. Appl. Phys.* **67** (1990) 2919.
85. B. TUCK and A. HOOPER, *J. Mater. Sci.* **11** (1976) 491.
86. P. AMBREE, A. HANGLEITER, M. H. PILKUHN and K. WANDEL, *Appl. Phys. Lett.* **56** (1990) 931.
87. E. A. POLTORATSKII and V. M. STUCHEBNIKOV, *Soviet Phys. Solid State* **8** (1966) 770.
88. M. ILEGEMS, *J. Appl. Phys.* **48** (1977) 1278.
89. W. V McLEVIGE, K. V. VAIDYANATHAN, B. G. STREETMAN, M. ILEGEMS, J. COMAS and L. PLEW, *Appl. Phys. Lett.* **33** (1978) 127.
90. J. N. MILLER, D. M. COLLINS and N. J. MOLL, *ibid.* **46** (1985) 960.
91. H. G. ROBINSON, M. D. DEAL and D. A. STEVENSON, *ibid.* **56** (1990) 554.
92. P. ENQUIST, G. W. WICKS, L. F. EASTMAN and C. HITZMAN, *J. Appl. Phys.* **58** (1985) 4130.
93. P. A. HOUSTON, F. R. SHEPHERD, A. J. SPRINGTHORPE, P. MANDERVILLE and A MARGITTAI, *Appl. Phys. Lett.* **52** (1988) 1219.
94. J. E. CUNNINGHAM, T. H. CHIU, A. OURMAZD, W. JAN and T. Y. KUO, *J. Cryst. Growth* **105** (1990) 111.
95. E. F. SCHUBERT, J. M. KUO, R. F. KOPF, H. S. LUFTMAN, L. C. HOPKINS and N. J. SAUER, *J. Appl. Phys.* **67** (1990) 1969.
96. M. KAWABE, N. SHIMIZU, F. HASEGAWA and Y. NANNICHI, *Appl. Phys. Lett.* **46** (1985) 849.
97. R. L. S. DEVINE, C. T. FOXON, B. A. JOYCE, J. B. CLEGG and J. P. GOWERS, *Appl. Phys.* **A44** (1987) 195.
98. D. L. KENDELL, in "Semiconductors and Semimetals", Vol 4, edited by Willardson and Beer (Academic, New York, 1968) Ch. 3.
99. H. P. HO, I. HARRISON, N. BABA-ALI and B. TUCK, *J. Appl. Phys.* **69** (1991) 3494.
100. I. HARRISON, H. P. HO and N. BABA-ALI, *J. Electron. Mater.* **20** (1991) 449.
101. H. P. HO, I. HARRISON, N. BABA-ALI, B. TUCK and M. HENINI, *ibid.* **20** (1991) 649.
102. C. H. WU, K. C. HSIEH, G. E. HÖFLER, N. EL-ZEIN and N. HOLONYAK, *Appl. Phys. Lett.* **59** (1991) 1224.
103. M. B. SMALL, R. M. POTEMSKI, W. REUTER and R. GHEZ, *ibid.* **41** (1982) 1068.
104. R. W. KALISKI, D. W. NAM, D. G. DEPPE, N. HOLONYAK Jr, K. C. HSIEH and R. D. BURNHAM, *J. Appl. Phys.* **2** (1987) 998.
105. D. G. DEPPE, L. J. GUIDO and N. HOLONYAK Jr, *Mater. Res. Soc. Symp. Proc.* **126** (1988) 31.
106. R. T. CHEN and W. G. SPITZER, *J. Electron. Mater.* **10** (1981) 1085.
107. R. MURRAY, R. C. NEWMAN, M. J. L. SANGSTER, R. B. BEALL, J. J. HARRIS, P. J. WRIGHT, J. WAGNER and M. RAMSTEINER, *J. Appl. Phys.* **66** (1989) 2589.
108. W. M. THEIS and W. G. SPITZER, *ibid.* **56** (1984) 890.
109. H. ONO and R. C. NEWMAN, *ibid.* **66** (1989) 141.
110. J. MAGUIRE, R. MURRAY, R. C. NEWMAN, R. B. BEALL and J. J. HARRIS, *Appl. Phys. Lett.* **50** (1987) 516.
111. M. E. GREINER and J. F. GIBBONS, *ibid.* **44** (1984) 750.
112. *Idem., ibid.* **57** (1985) 5181.
113. D. G. DEPPE, N. HOLONYAK Jr, F. A. KISH and J. E BAKER, *Appl. Phys. Lett.* **50** (1987) 998.
114. D. G. DEPPE, N. HOLONYAK Jr and J. E. BAKER, *ibid.* **52** (1988) 129.
115. K. B. KAHEN, *J. Appl. Phys.* **66** (1989) 176.
116. K. L. KAVANGH, J. W. MAYER, C. W. MAGEE, J. SHEETS, J. TONG and J. M. WOODALL, *Appl. Phys. Lett.* **47** (1985) 1208.
117. S. YU, U. M. GÖSELE and T. Y. TAN, *J. Appl. Phys.* **66** (1989) 2952.
118. G. A. BARAFF and M. SCHLUTER, *Appl. Phys. Lett.* **55** (1985) 1327.
119. K. H. LEE, D. A. STEVENSON and M. D. DEAL, *J. Appl. Phys.* **68** (1990) 4008.
120. J. LEE, L. WEI, S. TANIGAWA and M. KAWABE, *ibid.* **68** (1990) 5571.
121. M. KAWABE, N. MATSUURA, N. SHIMIZU, F. HASEGAWA and Y. NANNICHI, *Jpn. J. Appl. Phys.* **23** (1984) L623.
122. K. MEEHAM, P. GAVRILOVIC, N. HOLONYAK Jr, R. D. BURNHAM and R. L. THORNTON, *Appl. Phys. Lett.* **46** (1985) 75.
123. P. MEI, S. A. SCHWARZ, T. VENKATESAN, C. L.

SCHWARTZ, J. P. HARBISON, L. FLOREZ, N. D. THEODORE and C. B. CARTER, *ibid.* **53** (1988) 2560.
124. J. H. NEAVE, P. J. DOBSON, J. J. HARRIS, P. DAWSON and B. A. JOYCE, *Appl. Phys.* **A32** (1983) 195.
125. P. MEI, S. A. SCHWARZ, T. VENKATESAN, C. L. SCHWARTZ and E. COLAS, *Mater. Res. Soc. Symp. Proc.* **126** (1988) 71.
126. *Idem., J. Appl. Phys.* **65** (1989) 2165.
127. D. G. DEPPE, W. E. PLANO, J. E. BAKER, N. HOLONYAK Jr, M. J. LUDOWISE, C. P. KUO, T. D. FLETCHER, T. D. OSTENTOWSKI and M. G. CRAFORD, *Appl. Phys. Lett.* **53** (1988) 2211.
128. K. OGAWA and M. KAWABE, *Jpn. J. Appl. Phys.* 1 **29** (1990) 1240.
129. E. F. SCHUBERT, C. W. TU, R. F. KOPF, J. M. KUO and L. M. LUNARDI, *Appl. Phys. Lett.* **54** (1989) 2592.
130. E. F. SCHUBERT, J. B. STACK, T. H. CHUI and B. TELL, *ibid.* **53** (1988) 293.
131. L. J. GUIDO, N. HOLONYAK Jr, K. C. HSIEH, R. W. KALISKI, J. E. BAKER, D. G. DEPPE, R. D. BURNHAM, R. L. THORNTON and T. L. PAOLI, *J. Electron. Mater.* **16** (1987) 87.
132. T. H. CHIU, J. E. CUNNINGHAM, B. TELL and F. F. SCHUBERT, *J. Appl. Phys.* **64** (1988) 1578.
133. T. MIYAZAWA, Y. KAWAMURA and O. MIKAMI, *Jpn. J. Appl. Phys.* **27** (1988) L1731.
134. B. TUCK and M. H. BADAWI, *J. Phys. D: Appl. Phys.* **11** (1978) 2541.
135. D. SHAW, *Phys. Status Solid* i(a) **86** (1984) 629.
136. H. P. HO, I. HARRISON, N. BABA-ALI, B. TUCK and M. HENINI, *J. Mater. Sci: Mater. Electron.* **2** (1991) 137.
137. E. V. K. RAO, P. OSSART, F. ALEXANDRE and H. THIBIERGE, *Appl. Phys. Lett.* **50** (1987) 588.
138. D. G. DEPPE, W. E. PLANO, J. M. DALLESASSE, D. C. HALL, L. J. GUIDO and N. HOLONYAK Jr, *ibid.* **52** (1988) 825.
139. B. T. CUNNINGHAM, L. J. GUIDO, J. E. BAKER, J. S. MAJOR, N. HOLONYAK Jr and G. E. STILLMAN, *ibid.* **55** (1989) 687.
140. L. J. GUIDO, B. T. CUNNINGHAM, D. W. NMA, K. C. HSIEH, W. E. PLANO, J. S. MAJOR Jr, E. J. VESELY, A. R. SUGG, N. HOLONYAK Jr and G. E. STILLMAN, *J. Appl. Phys.* **67** (1990) 2179.
141. I. SZAFRANEK, M. SZAFRANEK, B. T. CUNNINGHAM, L. J. GUIDO, N. HOLONYAK Jr and G. E. STILLMAN, *ibid.* **68** (1990) 5615.
142. D. T. J. HURLE, *J. Phys. Chem. Solids* **40** (1979) 627.
143. A. B. YOUNG and G. L. PEARSON, *ibid.* **31** (1970) 517.
144. B. TUCK and R. G. POWELL, *J. Phys. D: Appl. Phys.* **14** (1981) 1317.
145. H. MATINO, *Solid-State Electron.* **17** (1974) 35.
146. E. V. K. RAO, H. THIBIERGE, F. BRILLOUET, F. ALEXANDRE and R. AZOULAY, *Appl. Phys. Lett.* **46** (1985) 867.
147. C. SHIEH, J. MANTZ, C. COLVARD, K. ALAVI, R. ENGLEMANN, Z. SMITH and S. WAGNER, *Superlatt. Microstr.* **4** (1988) 597.
148. J. S. MAJOR Jr, J. M. DALLESASSE, L. J. GUIDO, J. E. BAKER, W. E. PLANO, A. R. SUGG, E. J. VESELY, T. A. RICHARD and N. HOLONYAK Jr, *Appl. Phys. Lett.* **56** (1990) 1720.
149. N. BABA-ALI, I. HARRISON, B. TUCK, H. P. HO and M. HENINI, *Opti. Quantum Electron.* **23** (1991) S813.
150. J. J. COLEMAN, P. D. DAPKUS, C. G. KIRKPATRICK, M. D. CAMRAS and N. HOLONYAK Jr, *Appl. Phys. Lett.* **40** (1982) 904.
151. J. KOBAYASHI, M. NAKAJIMA, Y. BAMBA, T. FUKUNAGA, K. MATSUI, K. ISHIDA, H. NAKASHIMA and K. ISHIDA, *Jpn. J. Appl. Phys.* **25(2)** (1986) L385.
152. K. MATSUI, S. TAKATANI, T. FUKUNAGA, T. NARUSAWA, Y. BAMBA and H. NAKASHIMA, *ibid.* (1986) L391.
153. T. VENKATESAN, S. A. SCHWARZ, D. M. HWANG, R. BHAT, M. KOZA, H. W. YOON, P. MEI, Y. ARAKAWA and A. YARIV, *Appl. Phys. Lett.* **49** (1986) 701.
154. S. A. SCHWARZ, T. VENKATESAN, D. M. HWANG, H. W. YOON, R. BHAT and Y. ARAKAWA, *ibid.* **50** (1987) 281.
155. T. FUKUNAGA, K. ISHIDA, T. KURODA, K. MATSUI, T. NARUSAWA, T. MORITA, E. MIYAUCHI, HASHIMOTO and H. NAKASHIMA, in Institute of Physics Conference, Series No. 79 (1986) p. 439.
156. K. MATSUI, S. TAKAMORI, T. FUKUNAGA, T. NARUSAWA and H. NAKASHIMA, *Jpn. J. Appl. Phys.* **26(1)** (1987) 482.
157. E. A. DOBISZ, B. TELL, H. G. CRAIGHEAD, S. A. SCHWARZ, M. C. TAMARGO and J. P. HARBISON, *Mater. Res. Soc. Symp. Proc.* **77** (1987) 423.
158. K. ISHIDA, K. MATSUI, T. FUKUNAGA, J. KOBAYASHI, T. MORITA, E. MIYAUCHI and H. NAKASHIMA, *Appl. Phys. Lett.* **51** (1987) 109.
159. K. MATSUI, J. KOBAYASHI, T. FUKUNAGA, K. ISHIDA and H. NAKASHIMA, *Jpn. J. Appl. Phys.* **26** (1987) L1122.
160. M. UEMATSU and F. YANAGAWA, *ibid.* **26** (1987) L1407.
161. K. B. KAHEN, G. RAJESWARAN and S. TONG-LEE, *Appl. Phys. Lett.* **53** (1988) 1635.
162. S. TONG-LEE, G. BRAUNSTEIN, P. FELLINGER and G. RAJESWARAN, *Mater. Res. Soc. Symp. Proc.* **144** (1989) 489.
163. S. CHEN, S. TONG-LEE, G. BRAUNSTEIN and G. RAJESWARAN, *ibid.* **144** (1989) 463.
164. S. CHEN, S. TONG-LEE, G. BRAUNSTEIN, G. RAJESWARAN and P. FELLINGER, *ibid.* **147** (1989) 279.
165. P. GAVRILOVIC, D. G. DEPPE, K. MEEHAM, N. HOLONYAK Jr, J. J. COLEMAN and R. D. BURNHAM, *Appl. Phys. Lett.* **47** (1985) 130.
166. Y. HIRAYAMA, Y. SUZUKI and H. OKAMOTO, *Jpn. J. Appl. Phys.* **24** (1985) 1498.
167. J. RALSTON, G. W. WICKS, L. F. EASTMAN, B. C. DECOOMAN and C. B. CARTER, *J. Appl. Phys.* **59** (1985) 120.
168. J. CIBERT, P. M. PETROFF, D. J. WERDER, S. J. PEARTON, A. C. GOSSARD and J. H. ENGLISH, *Appl. Phys. Lett.* **49** (1986) 223.
169. E. A. DOBISZ, B. TELL, H. G. CRAIGHEAD and M. C. TAMARGO, *J. Appl. Phys.* **60** (1986) 4150.
170. K. KASH, B. TELL, P. GRABBLE, E. A. DOBISZ, H. G. CRAIGHEAD and M. C. TAMARGO, *ibid.* **63** (1988) 190.
171. P. MEI, T. VENKATESAN, S. A. SCHWARZ, N. G. STOFFEL, J. P. HARBISON, D. L. HART and L. A. FLOREZ, *Appl. Phys. Lett.* **52** (1988) 1487.
172. E. V. K. RAO, F. BRILLOUET, P. OSSART, Y. GAO, J. SAPRIEL and P. KRAUZ, in Institute of Physics Conference, Series No. 91 (1988) p. 553.
173. K. K. ANDERSON, J. P. DONNELLY, C. A. WANG, J. D. WOODHOUSE and H. A. HAUS, *Appl. Phys. Lett.* **53** (1988) 1632.
174. P. M. PETROFF *Mater. Res. Soc. Symp. Proc.* **104** (1988) 595.
175. B. ELAMN, E. S. KOTELES, P. MELMAN and C. A. ARMIENTO, *J. Appl. Phys.* **66** (1989) 2104.
176. S. CHEN, S. LEE, G. BRAUNSTEIN, K. Y. KO, L. ZHENG and T. Y. TAN, *Appl. Phys. Lett.* **55** (1989) 1194.
177. M. O'NEILL, A. C. J. H. BRYCE, J. H. MARSH, R. M. DE LA RUE, J. S. ROBERTS and C. JEYNES, *ibid.* **55** (1989) 1373.
178. P. P. PRONKO, A. W. McCORMICK, D. B. PATRIZIO, A. K. RAI, R. M. KOLBAS and B. S. FRANK, *Mater. Res. Soc. Proc.* **147** (1989) 297.
179. S. TONG LEE, S. CHEN, G. GRAUNSTEIN, K. KO, M. OTT and T. Y. TAN, *Appl. Phys. Lett.* **57** (1990) 389.
180. A. G. CULLIS, N. G. CHEW, C. R. WHITEHOUSE, D. C. JACOBSON, J. M. POATE and S. J. PEARTON, *ibid.* **55** (1989) 1211.
181. C. SHIEH, C. COLVARD, J. MANTZ, K. ALAVI and R. ENGELMANN, *Mater. Res. Soc. Symp. Proc.* **144** (1989) 531.
182. E. G. BITHELL, W. M. STOBBS, C. PHILLIPS, R. ECCLESTON and R. GWILLIAM, *J. Appl. Phys.* **67** (1990) 1279.

183. K. B. KAHEN, D. L. PETERSON and G. RAJESWAREN, *ibid.* **68** (1990) 2087.
184. H. LEIER, A. FORCHEL, G. HORCHER, J. HOMMEL, S. BAYER, H. ROTHFRITZ, G. WEIMANN and W. SCHLAPP, *ibid.* **67** (1990) 1805.
185. F. XIONG, T. A. TOMBRELLO, C. L. SCHWARTZ and S. A. SCHWARZ, *Appl. Phys. Lett.* **57** (1990) 896.
186. M. D. CAMRAS, J. J. COLEMAN, N. HOLONYAK Jr, K. HESS, P. D. DAPKUS and C. G. KIRKPATRICK, in Institute of Physics Conference Series No. 65 (1983) p. 233.
187. K. ISHIDA, T. TAKAMORI, K. MATSUI, T. FUKUNAGA, T. MORITA, E. MIYAUCHI, H. HASHIMATO and H. NAKASHIMA, *Jpn. J. Appl. Phys.* **25** (1986) L783.
188. G. W. ARNOLD, S. T. PICRAUX, P. S. PEERCY, D. R. MYERS and L. R. DAWSON, *Appl. Phys. Lett.* **45** (1984) 382.
189. D. R. MYERS, G. W. ARNOLD, I. J. FRITZ, L. R. DAWSON, R. M. BIEFELD, C. R. HILLS and B. L. DOYLE, *J. Electron. Mater.* **17** (1988) 405.
190. D. R. MYERS, R. M. BIEFELD, I. J. FRITZ, S. T. PICRAUX and T. E. ZIPPERIAN, *Appl. Phys. Lett.* **44** (1984) 1052.
191. E. V. K. RAO, P. OSSART, H. THIBIERGE, M. QUILLEC and P. KRAUZ, *ibid.* **57** (1990) 2190.
192. E. V. K. RAO, P. OSSART, H. THIBIERGE, M. QUILLEC, P. KRAUZ, presented at SSDM, Sendai, Japan, 1990.
193. I. J. PAPE, P. LIKAM WA, D. A. ROBERTS, J. P. R. DAVID, P. A. CLAXTON, P. N. ROBSON, in Institute of Physics Conference, Series No. 96 (1989) p. 397.
194. B. TELL, J. SHAH, P. M. THOMAS, K. F. BROWN-GOEBELER, A. DIGIOVANNI, B. I. MILLER and U. KOREN, *Appl. Phys. Lett.* **54** (1989) 1570.
195. B. TELL, B. C. JOHNSON, J. L. ZYSKIND, J. M. BROWN, J. W. SULHOFF, K. F. BROWN-GOEBELER, B. I. MILLER and U. KOREN, *ibid.* **52** (1988) 1428.
196. H. SUMIDA, H. ASAHI, S. J. YU, K. ASAMI, S. GONDA and H. TANOUE, *ibid.* **54** (1989) 520.
197. W. XIA, S. C. LIN, S. A. PAPPERT, C. A. HEWETT, M. FERNANDES, T. T. VU, P. K. L. YU and S. S. LAU, *ibid.* **55** (1989) 2020.
198. F. H. JULIEN, M. A. BRADLEY, E. V. K. RAO, M. RAZEGHI and L. GOLDSTEIN, *Opt. Quantum Electron.* **23** (1991) S847.
199. L. J. GUIDO, N. HOLONYAK Jr, K. C. HSIEH and J. E. BAKER, *Appl. Phys. Lett.* **54** (1989) 262.
200. A. H. van OMMEN, *J. Appl. Phys.* **54** (1983) 561.
201. N. A. STOLWIJK, M. PERRET, H. MEHRER, *Defect Diff. Forum* **59** (1988) 79.
202. L. PAVESI, D ARAUJO, N. H. KY, J. D. GANIERE, F. K. REINHART, P. A. BUFFAT and G. BURRI, *Opt. Quantum Electron.* **23** (1991) S789.
203. R. L. THORNTON, R. D. BURNHAM, T. L. PAOLI, N. HOLONYAK Jr and D. G. DEPPE, *J. Cryst. Growth* **77** (1986) 621.
204. Y. OHMORI, A. TATE and M. KOBAYASHI, *Jpn. J. Appl. Phys.* **26(1)** (1987) 1600.
205. D. G. DEPPE and N. HOLONYAK Jr, *J. Appl. Phys.* **64** (1988) R93.
206. R. L. THORNTON, W. J. MOSBY and H. F. CHUNG, *Appl. Phys. Lett.* (1988) 2669.
207. T. WOLF, C. L. SHIEH, R. ENGLEMANN, K. ALAVI, J. MANTZ, *ibid.* **55** (1989) 1412.
208. Y. SUZUKI, H. IWAMURA, T. MIYAZAWA, O. MIKAMI, *ibid.* **57** (1990) 2745.

Received and accepted 8 September 1992